Midwest States Pooled Fund Research Program
Fiscal Years 2013 (Years 23)
Research Project Number TPF-5(193) Supplement #56
NDOR Sponsoring Agency Code RPFP-13-MGS-3

INCREASED SPAN LENGTH FOR THE MGS LONG-SPAN GUARDRAIL SYSTEM PART III: FAILURE ANALYSIS

Submitted by

Sagheer A. Ranjha, Ph.D. MIEAust.
Postdoctoral Research Associate

Robert W. Bielenberg, M.S.M.E., E.I.T.
Research Engineer

John D. Reid, Ph.D.
Professor

Ronald K. Faller, Ph.D., P.E.
Research Associate Professor
MwRSF Director

MIDWEST ROADSIDE SAFETY FACILITY
Nebraska Transportation Center
University of Nebraska-Lincoln

Main Office
Prem S. Paul Research Center at Whittier School
Room 130, 2200 Vine Street
Lincoln, Nebraska 68583-0853
(402) 472-0965

Outdoor Test Site
4630 NW 36th Street
Lincoln, Nebraska 68524

Submitted to

MIDWEST STATES POOLED FUND PROGRAM
Nebraska Department of Roads
1500 Nebraska Highway 2
Lincoln, Nebraska 68502

MwRSF Research Report No. TRP-03-362-17

September 29, 2017

TECHNICAL REPORT DOCUMENTATION PAGE

1. Report No. TRP-03-362-17	2.	3. Recipient's Accession No.
4. Title and Subtitle Increased Span Length for the MGS Long-Span Guardrail System Part III: Failure Analysis		5. Report Date September 29, 2017
		6.
7. Author(s) Ranjha, S.A., Bielenberg, R.W., Reid, J.D., and Faller, R.K.		8. Performing Organization Report No. TRP-03-362-17
9. Performing Organization Name and Address Midwest Roadside Safety Facility (MwRSF) Nebraska Transportation Center University of Nebraska-Lincoln Main Office: Prem S. Paul Research Center at Whittier School Room 130, 2200 Vine Street Lincoln, Nebraska 68583-0853 Outdoor Test Site: 4630 NW 36th Street Lincoln, Nebraska 68524		10. Project/Task/Work Unit No. 11. Contract © or Grant (G) No. TPF-5(193) Supplement #56
12. Sponsoring Organization Name and Address Midwest States Pooled Fund Program Nebraska Department of Roads 1500 Nebraska Highway 2 Lincoln, Nebraska 68502		13. Type of Report and Period Covered Final Report: 2013 – 2017 14. Sponsoring Agency Code RPFP-13-MGS-3
15. Supplementary Notes Prepared in cooperation with U.S. Department of Transportation, Federal Highway Administration.		

16. Abstract

The objective of this research study was to review and analyze the system failure observed during crash testing of an increased span length for the MGS long-span guardrail system in test no. MGSLS-2. Test no. MGSLS-2 was a full-scale crash test conducted on the MGS long-span guardrail with a span length of 31¼ ft (9.5 m). This test utilized universal breakaway steel posts (UBSPs) adjacent to the long span in lieu of the controlled release terminal (CRT) wood posts used in previous long span systems.

An engineering analysis was undertaken to review the downstream end anchorage failure observed in test no. MGSLS-2. The analysis also compared critical aspects of the barrier performance with previous full-scale crash tests that had similar features or increased anchor loading. The results of this analysis and conclusions regarding potential causes of the anchor failure suggested that there was no identifiable root cause for anchor failure, but the pocketing and deflection suggest that the barrier system may have been pushed near its limits. It was noted that certain factors may have contributed to the anchor failure, including increased span length, location of the impact point, differences in the breakaway post behavior adjacent to the unsupported span, and natural variation in wood strength.

Following the analysis, several potential design modifications were noted for improving the barrier system and reducing the potential for end anchorage failure. However, it was noted that further analysis of these potential improvements, selection of a preferred design, and evaluation of the revised barrier system through full-scale crash tests will be required to fully evaluate the system to MASH TL-3 criteria.

17. Document Analysis/Descriptors Highway Safety, Crash Test, Roadside Appurtenances, Compliance Test, MASH, MGS, Midwest Guardrail System, Long Span, Guardrail, Failure, Analysis		18. Availability Statement No restrictions. Document available from: National Technical Information Services, Springfield, Virginia 22161	
19. Security Class (this report) Unclassified	20. Security Class (this page) Unclassified	21. No. of Pages 63	22. Price

DISCLAIMER STATEMENT

This report was completed with funding from the Federal Highway Administration, U.S. Department of Transportation and the Midwest States Pooled Fund Program. The contents of this report reflect the views and opinions of the authors who are responsible for the facts and the accuracy of the data presented herein. The contents do not necessarily reflect the official views or policies of the state highway departments participating in the Midwest States Pooled Fund Program nor the Federal Highway Administration, U.S. Department of Transportation. This report does not constitute a standard, specification, regulation, product endorsement, or an endorsement of manufacturers.

ACKNOWLEDGEMENTS

The authors wish to acknowledge several sources that made a contribution to this project: (1) the Midwest States Regional Pooled Fund Program funded by the Illinois Department of Transportation, Indiana Department of Transportation, Iowa Department of Transportation, Kansas Department of Transportation, Minnesota Department of Transportation, Missouri Department of Transportation, Nebraska Department of Roads, New Jersey Department of Transportation, Ohio Department of Transportation, South Dakota Department of Transportation, Wisconsin Department of Transportation, and Wyoming Department of Transportation for sponsoring this project; and (2) MwRSF personnel for constructing the barriers and conducting the crash tests.

Acknowledgement is also given to the following individuals who made a contribution to the completion of this research project.

Midwest Roadside Safety Facility

J.C. Holloway, M.S.C.E., E.I.T., Test Site Manager
K.A. Lechtenberg, M.S.M.E., E.I.T., Research Engineer
S.K. Rosenbaugh, M.S.C.E., E.I.T., Research Engineer
J.D. Schmidt, Ph.D., P.E., Research Assistant Professor
C.S. Stolle, Ph.D., Research Assistant Professor
M. Asadollahi Pajouh, Ph.D., Post-Doctoral Research Assistant
A.T. Russell, B.S.B.A., Testing and Maintenance Technician II
S.M. Tighe, Construction and Testing Technician I
D.S. Charroin, Construction and Testing Technician I
M.A. Rasmussen, Construction and Testing Technician I
E.W. Krier, Construction and Testing Technician II
M.T. Ramel, Construction and Testing Technician I
R.M. Novak, Construction and Testing Technician I
J.E. Kohtz, B.S.M.E., CAD Technician
E.L. Urbank, B.A., Research Communication Specialist
Undergraduate and Graduate Research Assistants

Illinois Department of Transportation

Priscilla A. Tobias, P.E., State Safety Engineer/Bureau Chief
Tim Sheehan, P.E., Safety Design Engineer
Paul L. Lorton, P.E., Safety Programs Unit Chief
Filiberto Sotelo, Safety Evaluation Engineer

Indiana Department of Transportation

Todd Shields, P.E., Maintenance Field Support Manager

Iowa Department of Transportation

Chris Poole, P.E., Roadside Safety Engineer
Brian Smith, P.E., Methods Engineer
Daniel Harness, Transportation Engineer Specialist

Kansas Department of Transportation

Ron Seitz, P.E., Bureau Chief
Scott King, P.E., Road Design Bureau Chief
Kelly Cool, P.E., Road Design Leader
Thomas Rhoads, P.E., Engineering Associate III, Bureau of Road Design

Minnesota Department of Transportation

Michael Elle, P.E., Design Standards Engineer
Michelle Moser, Assistant Design Standards Engineer

Missouri Department of Transportation

Ronald Effland, P.E., ACTAR, LCI, Non-Motorized Transportation Engineer
Joseph G. Jones, P.E., former Engineering Policy Administrator

Nebraska Department of Roads

Phil TenHulzen, P.E., Design Standards Engineer
Jim Knott, P.E., State Roadway Design Engineer
Mark Osborn, P.E., Secondary Roads Engineer
Jodi Gibson, Research Coordinator

New Jersey Department of Transportation

Dave Bizuga, P.E., Senior Executive Manager, Roadway Design Group 1

Ohio Department of Transportation

Don Fisher, P.E., Roadway Standards Engineer
Maria E. Ruppe, P.E., former Roadway Standards Engineer

South Dakota Department of Transportation

David Huft, P.E., Research Engineer
Bernie Clocksin, P.E., Lead Project Engineer

Wisconsin Department of Transportation

Jerry Zogg, P.E., Chief Roadway Standards Engineer
Erik Emerson, P.E., Standards Development Engineer
Rodney Taylor, P.E., Roadway Design Standards Unit Supervisor

Wyoming Department of Transportation

William Wilson, P.E., Architectural and Highway Standards Engineer

Federal Highway Administration

David Mraz, Division Bridge Engineer, Nebraska Division Office
Danny Briggs, Nebraska Division Office

TABLE OF CONTENTS

LIST OF FIGURES

LIST OF TABLES

1 INTRODUCTION

1.1 Problem Statement

Long-span guardrail systems have been recognized as an effective means of shielding low-fill culverts. These designs are popular due to their ability to safely shield the culvert while creating minimal construction effort and limiting culvert damage and repair when compared to other systems requiring post attachment to the top of the culvert [1-3]. However, previous long-span designs were limited by the need to use long sections of nested guardrail [4-9] to prevent rail rupture and the need for to provide large lateral offsets between the barrier and the culvert headwall [10-11]. The Midwest Guardrail System (MGS) long-span guardrail eliminated those two shortcomings by applying the benefits of the MGS to a long-span design [12-13]. The MGS long-span allowed for increased vehicle capture and stability through increased rail height, limited the potential for pocketing and wheel snag through the use of Controlled Release Terminal (CRT) posts adjacent to the unsupported span, and greatly increased the tensile capacity of the rail through the movement of splices away from the posts and the use of shallower post embedment. These features gave the MGS long-span guardrail the ability to perform safely without nested rail, and the minimal barrier offset made this new barrier a very functional and safe option for the protection of low-fill culverts.

In a previous study conducted by Midwest Roadside Safety Facility (MwRSF) [14], two full-scale crash tests were performed on the MGS long-span guardrail with a span length of 31.25 ft (9.5 m), as shown in Figure 1. Both crash tests utilized pickup trucks weighing approximately 5,000 lb (2,268 kg) as per *Manual for Assessing Safety Hardware* (MASH) [15] test designation no. 3-11. The target impact conditions for the test were a speed of 62 mph (100 km/h) and an angle of 25 degrees. The first test was conducted to evaluate the potential for vehicle instability by selecting a critical impact point (CIP) that maximized vehicle extension over the culvert and the potential for interaction of the front wheel of the pickup truck with the wing wall of the culvert. The second test was designed to evaluate the structural capacity of the system. These tests utilized Universal Breakaway Steel Posts (UBSPs) adjacent to the long span in lieu of the CRT wood posts previously tested [16].

The current report is based on the results and findings of the second full-scale crash test mentioned above. In test no. MGSLS-2, the CIP was selected near the downstream end of the unsupported span in order to evaluate the structural capacity of the system. After impacting the barrier system, the downstream anchor failed and caused the vehicle to penetrate the barrier system. Due to the failure of test no. MGSLS-2, further testing and design refinements are necessary on the MGS long-span guardrail for lengths over the 25 ft (7.6 m) span length.

Based on this failure event, an investigation was required to determine which potential factors may have caused the anchor failure. Thus, an anchor failure analysis was conducted for test no. MGSLS-2 in this report. The report discusses the factors effecting the failure of the anchor system and a brief discussion on the possible solutions for reducing the potential for anchor failure. Recommendations for potential design refinements and future testing were developed as well.

Test Installation

UBSP Post

Figure 1. MGS Long-Span Guardrail, 31.25-ft (9.5-m) Unsupported Span

1.2 Research Objectives

The objective of this research effort was to conduct an anchor failure analysis for test no. MGSLS-2, which was conducted as part of testing the increased span length for the MGS long-span guardrail. The various factors potentially affecting the end anchorage failure were identified and analyzed through the available data from test no. MGSLS-2 and other applicable full scale crash tests. Based on the failure analysis results, potential solutions to the anchor failure are provided.

1.3 Scope

The objective of the research was achieved by the completion of several tasks. First, the failure mechanisms of the downstream end anchorage in test no. MGSLS-2 were documented and reviewed. Next, possible contributing factors to the anchor failure were identified and compared with other previous full-scale crash tests of MGS systems. These factors included but were not limited to: increased span length, position of CIP, the use of UBSPs adjacent to unsupported guardrail span, soil forces, and wood strength variability. Finally, potential solutions and recommendations for further design refinement and testing were provided for reducing the potential for anchor failure.

2 LITERATURE REVIEW

In this chapter, the results of full-scale crash tests previously conducted on MGS are briefly described. The purpose was to review and compare these full-scale crash test results with test no. MGSLS-2 to provide insight into possible causes for the downstream end anchorage failure. Note that the selected tests were chosen because they are similar to the increased span length MGS long-span guardrail and/or represent significant loading of the guardrail system anchorages. The comparison of test results for MGS full scale crash tests is presented in Table 1. The anchor failure analysis results and discussions, along with the comparison with other MGS long-span guardrails, will be provided in subsequent chapters.

Table 1. Comparison of Test Results – MGS Full-Scale Crash Tests

Evaluation Criteria	MGSLS-1	MGSLS-2	LSC-1	LSC-2	MGSMP-1	MGSMIN-1	WIDA-1
Vehicle Test Inertial Mass, lb	4955	4912	4992	4984	4934	4956	5002
Impact Speed, mph	62.6	61.4	62.4	61.9	63.4	63.1	63
Impact Angle, deg	25.9	26.3	24.8	24.9	25.3	24.9	26.4
Exit Angle, deg	13.3	–	1	18.8	14	–	4.2
Dynamic Deflection, inches	61.6	164.2	92.2	77.5	49.0	42.2	390.6
Working Width, inches	64.6	–	93.4	83.9	50.1	48.8	390.6
Max. Roll, deg	-13.1	-15.65	–	–	11.79	6.5	10.2
Max. Pitch, deg	-4.0	16.62	–	–	-5.12	-5	4.5
OIV – Longitudinal, ft/s – Lateral, ft/s	-12.92 11.64	-13.22 3.16	-9.6 10.6	-16.1 13.4	-13.63 -14.08	-15.9 14.0	-14.56 -15.13
ORA – Longitudinal, g's – Lateral, g's	-15.76 6.13	-23.68 10.57	-6.48 5.91	-7.34 4.24	-10.29 -7.94	-8.1 5.7	-8.01 -6.31

2.1 Test No. MGSLS-1

The MGS long-span guardrail with increased unsupported span length was evaluated to MASH standards through two full-scale crash tests conducted under test designation no. 3-11 [14]. For test no. MGSLS-1, a CIP was selected that maximized the lateral extension of the vehicle over the culvert and promoted increased vehicle interaction with the downstream end of the culvert headwall. The barrier consisted of a 175-ft (53.3-m) long MGS system that incorporated a 31.25-ft (9.5-m) unsupported guardrail span with three UBSPs installed adjacent to each end of the unsupported span to reduce the potential for vehicle snag and rail pocketing. A trailing end

anchorage designed to replicate the capacity of a tangent guardrail terminal was used on each end of the system and consisted of BCT timber posts, anchor cable, and two foundation tubes connected by a ground strut. All posts were spaced at 75 in. (1,905 mm) on center. The 31.25 ft (9.5 m) unsupported span located near the center of the guardrail installation bridged a simulated concrete culvert. Test no. MGSLS-1 was selected for comparison with test no. MGSLS-2 because they were identical systems with different impact points. In test no. MGSLS-1, the 4,955 lb (2,248 kg) pickup truck impacted the MGS long-span guardrail at a speed of 62.7 mph (100.9 km/h), an angle of 25.3 degrees, and at a location 1¾ in. (44 mm) downstream of post no. 11, resulting in an impact severity of 124.1 kip-ft (168.2 kJ). After impacting the barrier system, the vehicle exited the system at a speed of 27.3 mph (44.0 km/h) and an angle of 13.3 degrees. The vehicle was successfully contained and smoothly redirected with moderate damage to both the barrier system and the vehicle. The dynamic deflection was 61.6 in (1,564 mm) and working width was 64.6 in (1,641 mm). All vehicle decelerations fell within the recommended safety limits established in MASH, and test no. MGSLS-1 was deemed successful according to the safety criteria of MASH test designation 3-11.

2.2 Test No. LSC-1

The original MGS long-span guardrail system was capable of traversing culverts with an unsupported span 25.0 ft (7.62 m) in length and was evaluated through two full-scale crash tests, test nos. LSC-1 and LSC-2 [12-13]. Test no. LSC-1 was intended to evaluate the system at a critical impact point that maximized the potential for pocketing, wheel snag, and rail rupture. The MGS long-span guardrail system in test no. LSC-1 consisted of 181.25 ft (55.25 m) of standard 12-gauge W-beam guardrail supported by steel posts and six CRT posts. The tested barrier was similar to the system tested in test no. MGSLS-2 except for a shorter unsupported span length and the use of CRT posts rather than UBSPs adjacent to the unsupported span. For test no. LSC-1, the simulated culvert headwall consisted of a 9.0-in. thick x 48.0-in. tall (229-mm thick x 1,219-mm tall) reinforced concrete wall installed 12.0 in. (305 mm) behind the back of the CRT posts in the system. Anchorage systems similar to those used on tangent guardrail terminals were utilized on both the upstream and downstream ends of the guardrail system. The entire system was constructed with twenty-six guardrail posts. Dissimilarities between test no. LSC-1 and test no. MGSLS-2 included different impact points and terrain adjacent to the culvert. Test no. MGSLS-2 impacted approximately 6 ft (1.83 m) closer to the first post on the downstream end of the unsupported span. LSC-1 was evaluated on level terrain while MGSLS-2 had a 3:1 slope offset 2 ft (610 mm) behind the system. In test no. LSC-1, a 4,992-lb (2,264-kg) pickup truck impacted the MGS long-span guardrail system at a speed of 62.5 mph (100.5 km/h) and at an angle of 24.8 degrees. Vehicle impact occurred 8.0 ft (2.44 m) downstream from the centerline of post no. 13. In test no. LSC-1, showed that the MGS long-span guardrail adequately contained and redirected the vehicle with controlled lateral displacements of the guardrail. The dynamic deflection was 92.2 in (2,342 mm) and the working width was 93.4 in (2,372 mm). Therefore, test no. LSC-1 conducted on the MGS long-span guardrail system was deemed successful according to the safety criteria of MASH test designation no. 3-11.

2.3 Test No. LSC-2

Test no. LSC-2 was conducted to evaluate the hazard posed by an impact that maximized the interaction between the vehicle and the culvert wing walls. The design of the MGS long-span

guardrail used for test no. LSC-1 remained unchanged for test no. LSC-2, but modifications were made to the design of the culvert and the lateral offset between the guardrail and the culvert headwall. For test no. LSC-2, the simulated culvert was installed flush with the back of the CRT posts in the system and a 3:1 slope was implemented 2 ft (610 mm) behind the guardrail posts. In test no. LSC-2, a 4,984-lb (2,261-kg) pickup truck impacted the MGS long-span guardrail system at a speed of 61.9 mph (99.6 km/h) and at an angle of 24.9 degrees at a CIP chosen to maximize the interaction of the impacting vehicle with the walls of the culvert. Vehicle impact occurred 41.24 ft (12.57 m) upstream from the centerline of post no. 14. Test no. LSC-2 demonstrated that the MGS long-span guardrail adequately contained and redirected the vehicle with controlled lateral displacements of the guardrail. The dynamic deflection was 77.5 in (1,969 mm) and the working width was 83.9 in (2,131 mm). It was noted that the occupant impact velocities (OIV) and occupant ride-down decelerations (ORD) were within the suggested limits. Therefore, test no. LSC-2 conducted on the MGS long-span guardrail system was deemed successful according to the safety criteria of MASH test designation no. 3-11 [12].

2.4 Test No. MGSMP-1

The test installation for MGS with one omitted post consisted of 182 ft – 3½ in. (55.6 m) of standard 31-in. tall W-beam guardrail supported by steel posts. A single full-scale crash test, test no. MGSMP-1, was conducted with the 2270P pickup truck to evaluate the MGS with one omitted post in accordance with MASH test no. 3-11. The test installation utilized standard 6-ft (1.8-m) long steel guardrail posts with 12-in. (305-mm) deep blockouts. All posts were spaced at 75 in. (1,905 mm) on center, except for a single 150-in. (3,810-mm) span located near the center of the guardrail installation, which represented the omitted post in the otherwise standard MGS. Test no. MGSMP-1 was chosen for comparison with test no. MGSLS-2 based on its use of an unsupported span and the potential for similar increases in rail load and barrier pocketing. Test no. MGSMP-1 consisted of a 4,934-lb (2,238-kg) pickup truck impacting the MGS with an omitted post at a speed of 63.4 mph (102.1 km/h) and an angle of 25.3 degrees. The vehicle was contained and smoothly redirected with only moderate damage sustained by the system and the vehicle. The dynamic deflection was 49 in (1,245 mm) and working width was 50.1 in (1,273 mm). The vehicle remained upright, and all vehicle decelerations were within the recommended occupant risk limits [17].

2.5 Test No. MGSMIN-1

The recommended minimum length for the standard MGS had historically been 175 ft (55.3 m) based on crash testing according to NCHRP Report No. 350 and MASH. A research study was undertaken to evaluate the effects of reducing the system length of the MGS. The research study included one full-scale crash test, test no. MGSMIN-1, in which a Dodge Ram pickup truck impacted a 75-ft (22.9-m) long MGS. This test was selected for comparison with test no. MGSLS-2 based on the potential for increased end anchor loading in the reduced length system.

Test no. MGSMIN-1, was performed on the MGS with a top rail mounting height of 31 in. (787 mm). The system incorporated 72-in. (1,829-mm) long, W6x8.5 (W152x12.6) steel posts with an embedment depth of 40 in. (1,016 mm). End anchorage systems, similar to those used on tangent guardrail terminals, were utilized on both the upstream and downstream ends of the guardrail system. The test consisted of a 4,956-lb (2,248 kg) pickup truck impacting the barrier

system at a speed of 63.1 mph (101.6 km/h) and at an angle of 24.9 degrees. Initial vehicle impact was to occur at the center line of post no. 4, and the actual point of impact was 4 in. (102 mm) downstream of post no. 4. During the test, the vehicle was contained and smoothly redirected without any significant snagging or pocketing. The maximum permanent set and dynamic deflections were 36⅜ in. (924 mm) and 42.2 in. (1,072 mm), respectively. The working width of the system was 48.8 in. (1,240 mm). The test results were found to meet all the MASH safety requirements for test designation no. 3-11 [18].

2.6 Test No. WIDA-1

A non-proprietary, downstream end anchorage system for 31-in. (787-mm) tall guardrail was crash tested and evaluated according to the MASH impact safety standards [19]. The anchorage was an adaptation of the original modified BCT anchor system, but it was installed tangent. It consisted of two BCT timber posts set into 6-in. wide x 8-in. deep x 72-in. long (152-mm x 203-mm x 1,829-mm) steel foundation tubes. The two steel foundation tubes were connected at the ground line through a strut and yoke assembly. A ¾-in. (19-mm) diameter 6x19 wire rope connected the back of the W-beam to the bottom of the end post. The test installation consisted of 181 ft – 3 in. (55.2 m) of MGS along with the end anchorage system noted previously on each end. The system was constructed with twenty-nine posts. Post nos. 3 through 27 were galvanized, ASTM A36, W6x8.5 (W152x12.6) sections measuring 72 in. (1,829 mm) longTwo full-scale crash tests were performed on the system under MASH modified designation no. 3-37. Test no. WIDA-1 was conducted with a 5,172-lb (2,346-kg) pickup truck to identify the end of the LON, while test no. WIDA-2 was conducted with a 2,619-lb (1,188-kg) small passenger car to assess any potential vehicle instability. Test No. WIDA-1 was selected for comparison with test no. MGSLS-2 based on the potential for increased anchor loads due to impact of a 2270P vehicle near the end of the system.

In test no. WIDA-1, the 2270P vehicle impacted the 31-in. (787-mm) high MGS barrier at the centerline of the sixth post upstream from the trailing-end terminal (i.e., post no. 24) with an initial impact speed and angle of 63.0 mph (101.4 km/h) and 26.4 degrees, respectively. Both the downstream anchor BCT wood posts fractured before direct contact with the 2270P pickup truck could occur. Due to the early fracture of the end post, the anchor cable was released before the vehicle became parallel to the barrier system. After the BCT wood posts fractured, the pickup truck continued yawing while proceeding downstream, with the rear wheels skidding and the front wheels still in contact with the ground and redirecting the vehicle. The front wheels realigned after the vehicle was downstream of the end post, and the pickup truck proceeded along a straight path until eventually coming to a complete stop facing downstream. The dynamic deflection was 390.6 in (9921 mm) and the working width was 390.6 in (9921 mm). Test no. WIDA-1 was determined to be acceptable according to the MASH safety performance criteria for modified test designation no. 3-37.

3 ANCHOR FAILURE ANALYSIS OF TEST NO. MGSLS-2

An engineering analysis was undertaken to review the anchor failure observed in test no. MGSLS-2. The analysis reviewed a variety of factors that may have contributed to the anchor failure. The analysis also compared critical aspects of the barrier performance with previous full-scale crash tests that had similar features or increased anchor loading. The results of this analysis and conclusions regarding potential causes of the anchor failure are presented in the subsequent sections. Possible modifications to the barrier system to mitigate the anchor failure will be presented the next chapter.

The original MASH MGS long-span guardrail (LSC test series) provided the capability to span unsupported lengths up to 25 ft with wood CRT post near the span. The MGS long-span guardrail (MGSLS tests) consisted of a 31.25-ft span MGS with the wood CRT posts near the span replaced by UBSPs. The test installation layout for test no. MGSLS-2 is shown in Figure 2. Full system details can be found in the research report [14]. Two critical impact points CIP's were determined for this system and tested with the 2270P truck. The only dissimilarity between test nos. MGSLS-1 and MGSLS-2 was the impact location. For test no. MGSLS-2, the CIP was selected to maximize the potential for pocketing, wheel snag, and rail rupture [16]. The test installation for the MGS long-span guardrails was composed of 175 ft (53.3 m) of standard W-beam guardrail supported by BCT timber posts, standard steel posts, UBSPs, and the concrete culvert. All posts were spaced at 75 in. (1,905 mm) on center. A single 31.25 ft (9.5 m) unsupported span located near the center of the guardrail installation bridged a simulated concrete culvert.

3.1 Anchor Components in MGSLS-2

The MGS long-span end-anchorage system consists of the following components, as shown in Figure 3.

1. Two MGS BCT posts
2. Soil foundation tubes
3. Cable anchor assembly
4. Guardrail
5. C-channel ground line strut
6. Load cell assembly

The MGS BCT posts were installed in steel soil foundation tubes, which were embedded to a depth of 70 in. (1778 mm). A BCT cable assembly was attached to the post by inserting a swaged end of the cable into the BCT hole and through a bearing plate, and attached to the guardrail using a cable anchor bracket. The guardrail was attached to the BCT posts with a top mounting height of 31 in. (787 mm). A bent plate, C-shape, ground line strut was used to connect the two soil foundation tubes [20]. For test no. MGSLS-2, anchor cable on each end of the system was spliced with a 50-kip load cell assembly. The load cell had been spliced into the anchor cable in a variety of past guardrail tests with no adverse effect on anchor capacity, and the incorporation of the load cell provided valuable anchor load data.

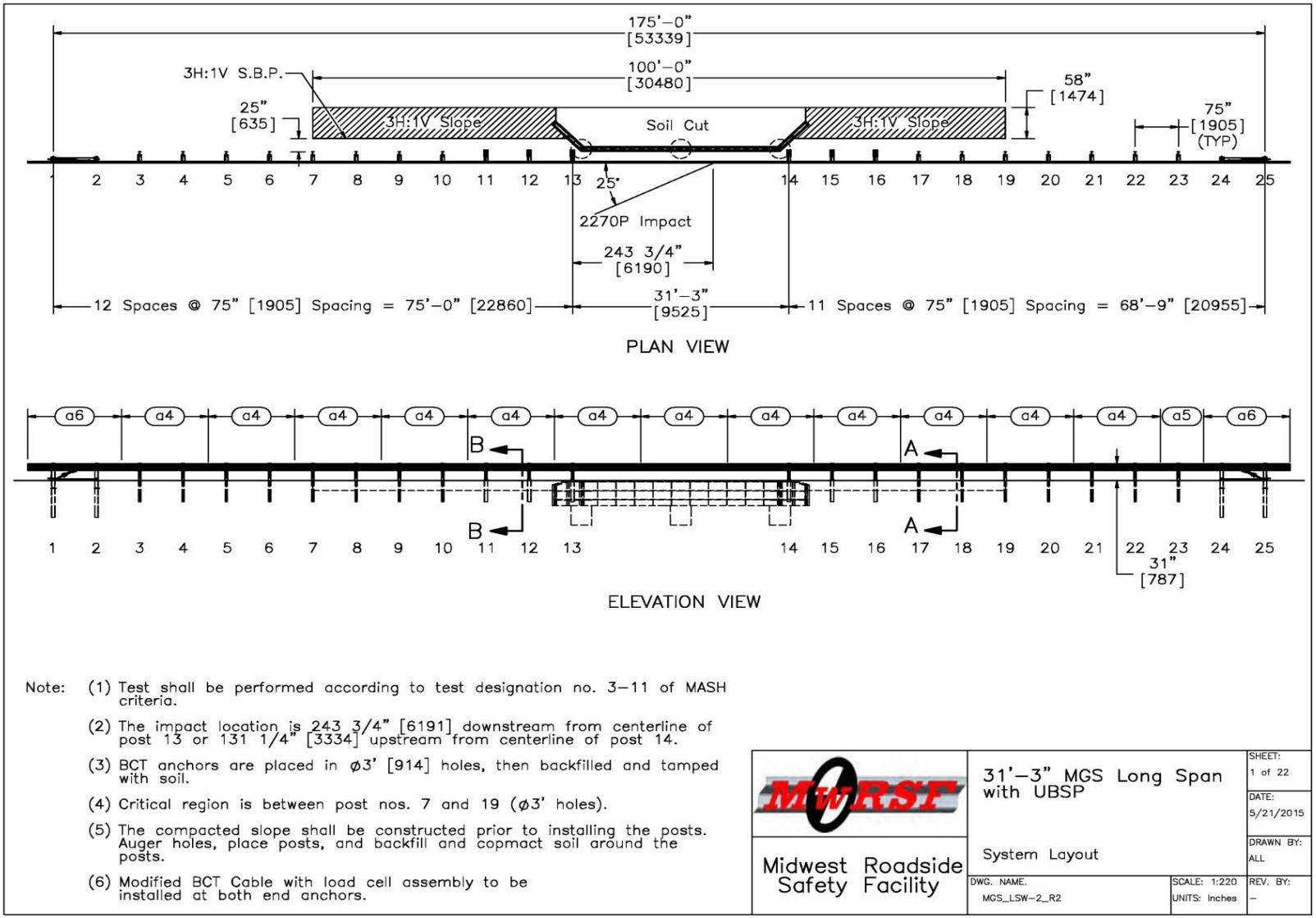

Figure 2. Test Installation Layout, Test No. MGSLS-2

3.2 MGSLS-2 Anchor Failure

In test no. MGSLS-2, the 4,912-lb (2,228-kg) pickup truck impacted the MGS long-span guardrail at a speed of 61.4 mph (98.8 km/h), an angle of 26.3 degrees, and at a location 239.71 in. (6,093 mm) downstream from post no. 13, which resulted in an impact severity of 110.7 kip-ft (150.0 kJ). During the test, the downstream anchor system failed and allowed the rail to disengage from the posts and become wrapped around the vehicle. The vehicle penetrated beyond the barrier and came to rest 17 ft – 9 in. (5.4 m) behind the system and 44 ft – 9 in. (13.6 m) downstream from the point of impact. A summary of the sequential photographs is shown in Figures 4 and 5.

Following the initial impact of the 2270P vehicle with the W-beam rail, the W-beam rail captured the pickup truck and began to redirect the vehicle. The guardrail deflected laterally, which caused the first UBSP downstream of impact, post no. 14, to fracture at 0.078 sec after impact. The vehicle continued to be redirected, and deflected the guardrail and the second UBSP downstream of impact, post no. 15, laterally.

As the vehicle was redirected, the BCT posts at the downstream end anchorage, post nos. 24 and 25, were deflected longitudinally upstream due to tensile loads in the guardrail and the cable anchorage. Vertical cracking in post no. 24 was initiated at approximately 0.095 sec due to longitudinal loading of the post through the post bolt connecting the post to the guardrail, as shown in Figure 6 and Figure 7. As loading of the downstream anchorage continued, a diagonal crack initiated near the top of the BCT cable anchor plate on the downstream face of post no. 25. This crack propagated down to the hole in the base of the BCT post and caused complete fracture and release of post no. 25 at approximately 0.140 sec after impact. Following the release of the cable anchorage at post no. 25, post no. 24 fractured and released as well. Release of the downstream end anchorage caused the guardrail to lose tensile on the downstream end of the system and allowed the 2270P vehicle to penetrate into the barrier system in an uncontrolled manner.

Wood post damage included fracturing, gouging, and displacement of posts. Post no. 1 had gouging on the front face due to rail contact. Post no. 2 split vertically along the height of the post through the guardrail bolt hole on the front side. Post nos. 24 and 25 fractured at the ground line and post no. 24 also split along the vertical plane of the centerline of the post. Post no. 25 had a 7½-in. (191-mm) deep by 3-in. (76-mm) wide crack located 2¼ in. (57 mm) downward from the top of the back face of the post, as well as a 3-in. (76-mm) diameter dent on the back downstream face of the post. The post-test photographs of the end anchorage system for test no. MGSLS-2 are shown in Figure 8. No knots or asperities were observed in the fracture region of post no. 25, as shown in Figure 9.

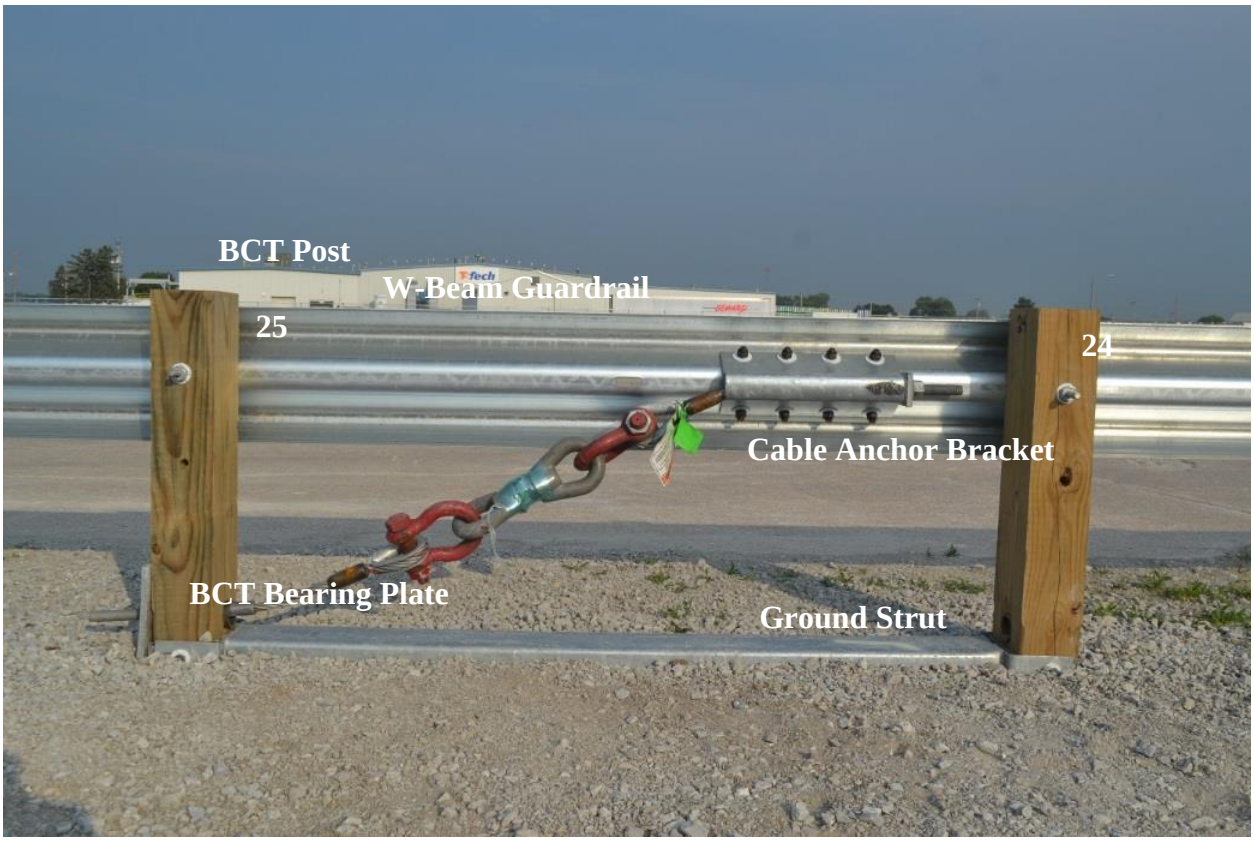

Figure 3. Long-Span End-Anchorage System, Test No. MGSLS-2

3.3 Analysis of Parameters Related to Downstream Anchorage Failure

Following the failure of test no. MGSLS-2, the researchers analyzed a variety of parameters related to the downstream anchor failure in order to provide insight into the cause of the failure. These parameters are listed below.

1. Loading and deflection of the end anchorage
2. Behavior of the breakaway posts adjacent to the unsupported span prior to failure
3. Rail pocketing
4. Location of the vehicle impact point
5. Barrier deflection prior to failure
6. Rail release from the posts prior to failure
7. Vehicle trajectory prior to failure
8. Soil strength
9. Variability of wood

Each of these parameters was investigated with respect to test no. MGSLS-2. In addition, similar parameters from other relevant MGS full-scale crash tests were analyzed for comparison purposes.

It should also be noted that test no. MGSLS-2 had a 3:1 slope installed at a 2 ft (610 mm) offset from the back of the system posts, while test no. LSC-1 was installed on level terrain. The difference in grading behind the two systems was not believed to be a factor in the end anchorage failure as the anchor broke prior to vehicle engagement with the slope and sufficient backfill was provided behind the posts prior to the 3:1 slope to ensure that post-soil forces would not be affected by the presence of the slope.

The following full-scale crash tests of the MGS were utilized for comparison, as noted in Chapter 2.

1. Increased MGS long span – MGSLS-1
2. MGS long span – LSC-1, LSC-2
3. MGS minimum length – MGSMIN-1
4. MGS downstream anchor – WIDA-1
5. MGS omitted post – MGSMP-1

The results of the analysis of each of the anchor failure parameters investigated are detailed in the subsequent sections.


0.000 sec


0.036 sec


0.084 sec


0.132 sec


0.180 sec


0.412 sec


0.000 sec


0.108 sec


0.216 sec


0.318 sec


0.730 sec


1.104 sec

Figure 4. Sequential Photographs, Test No. MGSLS-2


0.000 sec


0.000 sec


0.030 sec


0.076 sec


0.094 sec


0.152 sec


0.190 sec


0.266 sec


0.554 sec


0.400 sec


1.840 sec


0.744 sec

Figure 5. Sequential Photographs, Test No. MGSLS-2

Time = 0.000 Sec

Time = 0.100 Sec

Figure 6. Sequential Photographs of Downstream End Anchorage, Test No. MGSLS-2

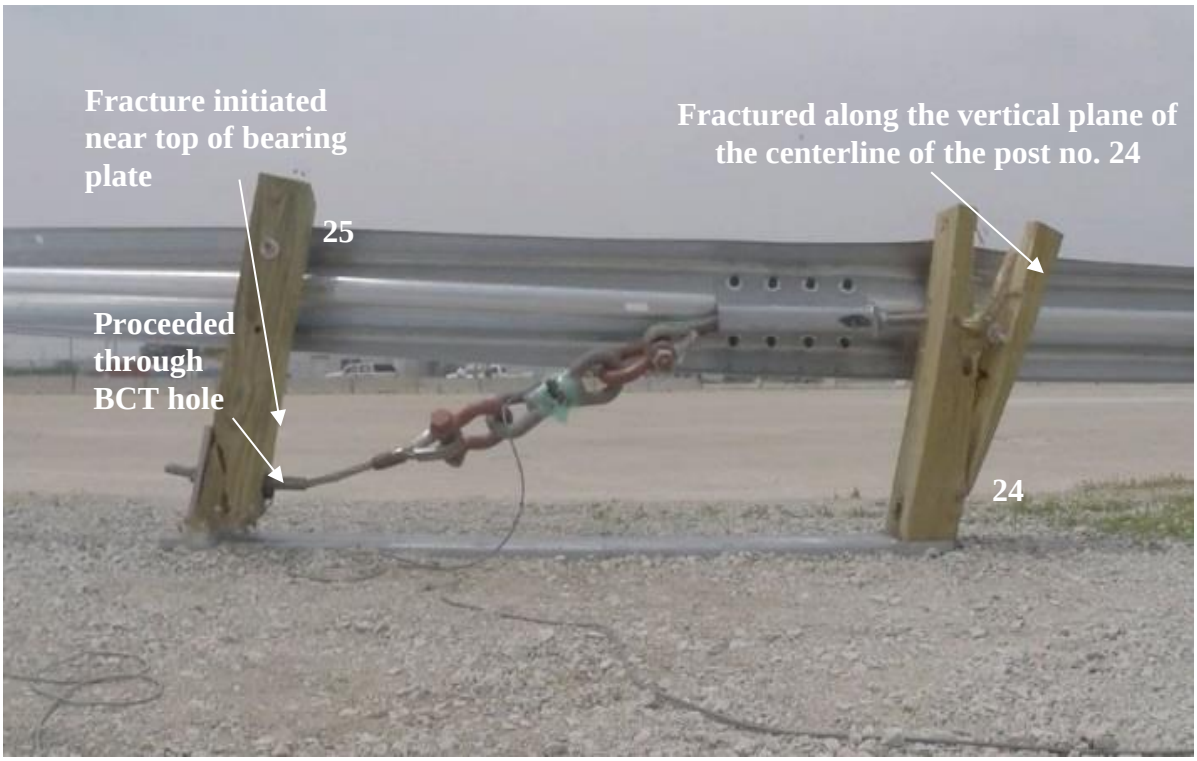

Time = 0.150 Sec

Time = 0.175 Sec

Figure 7. Sequential Photographs of Downstream End Anchorage, Test No. MGSLS-2, Cont.

Figure 8. Post-Test Photographs of End Anchorage System, Test No. MGSLS-2

Figure 9. Post No. 25 Damage, Test No. MGSLS-2

3.3.1 Anchor Loads and Deflection

Analysis of the anchor failure began with a comparison the load and deflection of the downstream end anchorage in test no. MGSLS-2 with other available data from tests of similar end anchorages. Figures 11 through 18 show a sequential comparison between the loading and deflection of the downstream end anchorage in test no. MGSLS-2 and other similar anchorages under full-scale testing impacts with 2270P vehicles, including the upstream end anchorages from test nos. MGSLS-2, MGSMP-1, and MGSMIN-1 and the downstream end anchorage from MGSLS-1. Review of the sequential images found that all of the anchorages displayed similar deflection behavior in terms of deflection downstream due to the tensile loading of the W-beam rail. The vertical splitting of post no. 24 in test no. MGSLS-2 was not a singular event as test nos. MGSLS-2 and MGSMP-1 demonstrated similar behavior on the upstream anchors, but did not fail. Motion of the cable end plate was also reviewed for all of the tests and no abnormal deflection or rotation of the cable end plate was noted in test no. MGSLS-2 prior to the anchorage failure as compared to the other tests.

Film analysis was used to compare the deflection angle of the posts from vertical as the anchorages were loaded, as shown in Figures 18 and 19. Note that the deflection angle of the second BCT post from vertical for in test no. MGSLS-2 was not measured after the vertical splitting of the anchor post, and the angle of the first BCT post in test no. MGSLS-2 increased rapidly after 0.120 sec due to the formation of the crack near the top of the cable anchor plate noted previously. Comparison of the deflection angles found that the deflection of the BCT posts in the downstream anchor from test no. MGSLS-2 was not markedly different or excessive as compared to previous tests without anchor failure prior to fracture of the anchor posts.

Anchor load and deflection were also compared. The upstream end anchorages in test nos. MGSLS-2, MGSMP-1, and MGSMIN-1 as well as the downstream anchorages in test nos. MGSLS-1 and MGSLS-2 were instrumented with 50-kip tension load cells spliced in line with the end anchor cable. Additionally, string pots were attached to the base of the foundation tube on the final post for measurement of linear displacement of the anchorage in the longitudinal direction. These transducers allowed for comparisons of the load and deflection of these anchorages.

The anchor loading of failed test no. MGSLS-2 was reviewed first. Anchor load versus time and anchor load versus foundation tube deflection for the upstream end anchorage and the downstream end anchorage that failed in test no. MGSLS-2 are shown in Figure 20 and Figure 21, respectively. The downstream anchorage in test no. MGSLS-2 developed a peak load of 27.5 kips (122.3 kN) at approximately 1.6 in. (41 mm) of deflection prior to failure of post no. 25 and release of the anchor cable. The upstream anchorage in test no. MGSLS-2 developed a peak load of 24.4 kips (108.5 kN) at approximately 1.8 in. (46 mm) of deflection, but the upstream end anchorage did not show any signs of anchor failure. Thus, similar load and deflection were observed in the upstream and downstream anchorages, but only the downstream anchorage failed.

Time = 0.000 Sec

MGSLS-2 Downstream

MGSLS-2 Upstream

MGSLS-1 Downstream

MGSMP-1 Upstream

MGSMIN-1 Upstream

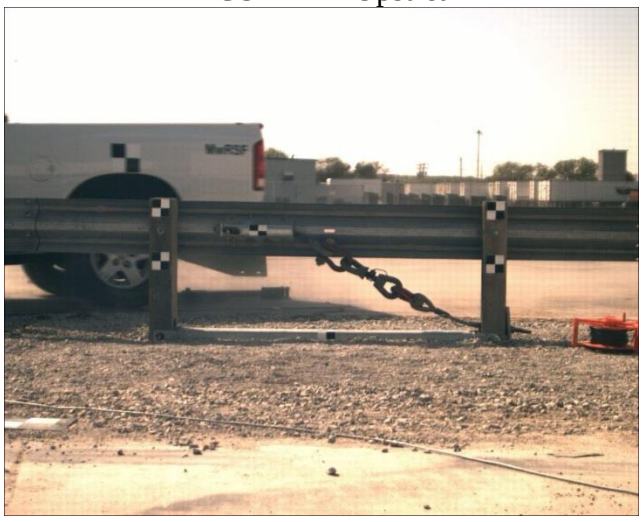

Figure 10. End Anchorage Sequential View Comparison of MGS Tests

Time = 0.025 Sec

MGSLS-2 Downstream

MGSLS-2 Upstream

MGSLS-1 Downstream

MGSMP-1 Upstream

MGSMIN-1 Upstream

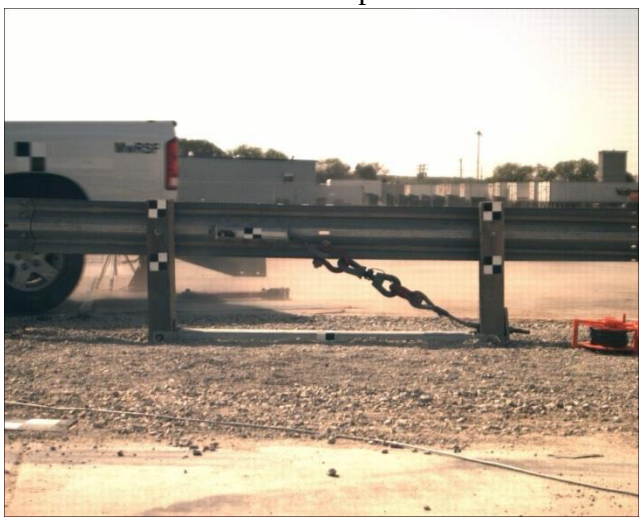

Figure 11. End Anchorage Sequential View Comparison of MGS Tests

Time = 0.050 Sec

MGSLS-2 Downstream

MGSLS-2 Upstream

MGSLS-1 Downstream

MGSMP-1 Upstream

MGSMIN-1 Upstream

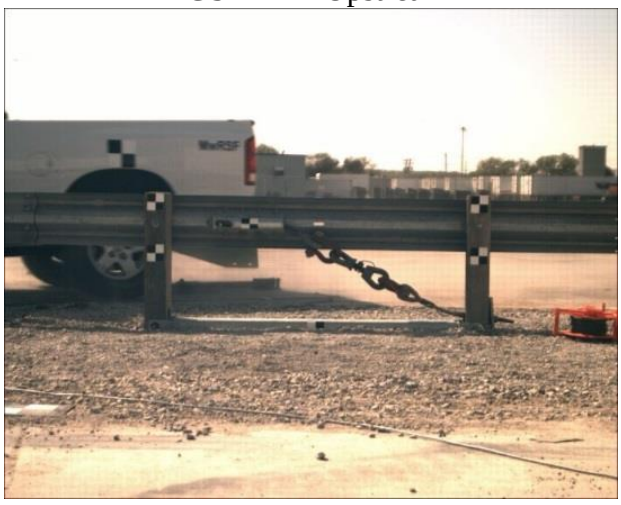

Figure 12. End Anchorage Sequential View Comparison of MGS Tests

Time = 0.075 Sec

MGSLS-2 Downstream

MGSLS-2 Upstream

MGSLS-1 Downstream

MGSMP-1 Upstream

MGSMIN-1 Upstream

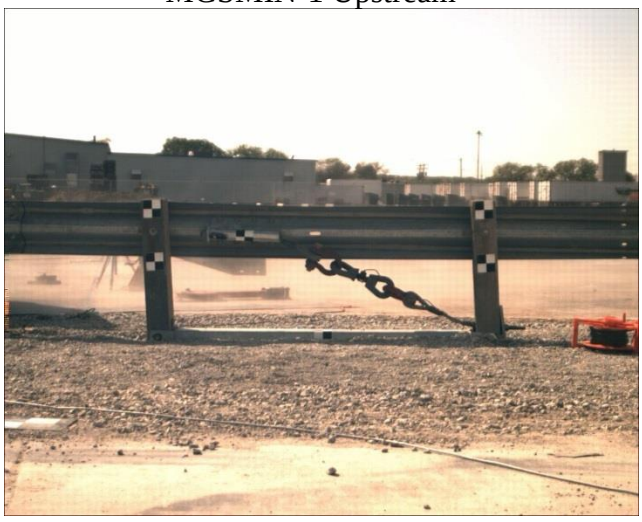

Figure 13. End Anchorage Sequential View Comparison of MGS Tests

Time = 0.100 sec

MGSLS-2 Downstream

MGSLS-2 Upstream

MGSLS-1 Downstream

MGSMP-1 Upstream

MGSMIN-1 Upstream

Figure 14. End Anchorage Sequential View Comparison of MGS Tests

Time = 0.125 sec

MGSLS-2 Downstream

MGSLS-2 Upstream

MGSLS-1 Downstream

MGSMP-1 Upstream

MGSMIN-1 Upstream

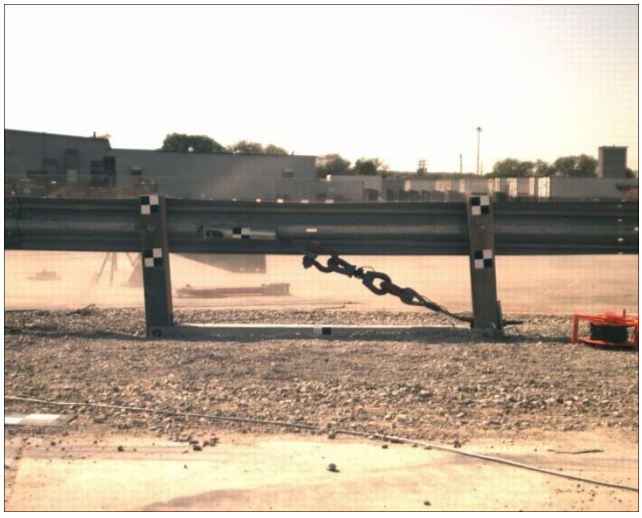

Figure 15. End Anchorage Sequential View Comparison of MGS Tests

Time = 0.150 sec

MGSLS-2 Downstream

MGSLS-2 Upstream

MGSLS-1 Downstream

MGSMP-1 Upstream

MGSMIN-1 Upstream

Figure 16. End Anchorage Sequential View Comparison of MGS Tests

Time = 0.175 sec

MGSLS-2 Downstream

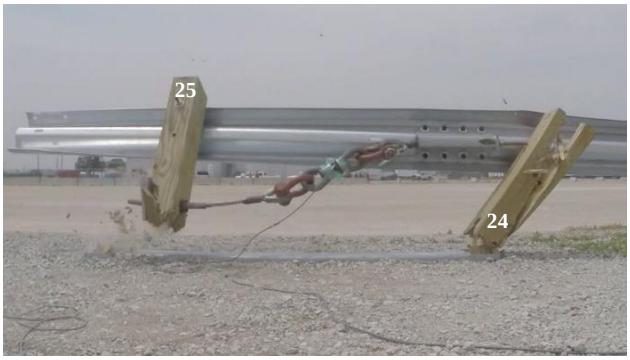

MGSLS-2 Upstream

MGSLS-1 Downstream

MGSMP-1 Upstream

MGSMIN-1 Upstream

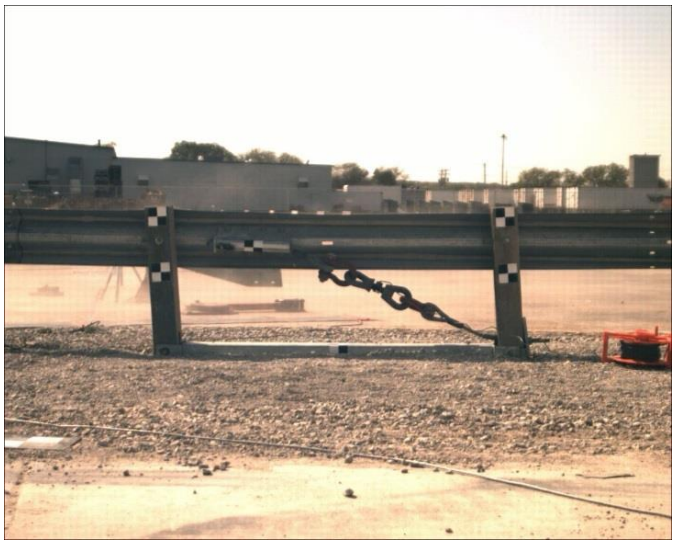

Figure 17. End Anchorage Sequential View Comparison of MGS Tests

Failure of an instrumented end anchorage assembly had not been observed in any full-scale crash tests prior to test no. MGSLS-2. However, dynamic component testing of end anchorages was conducted as part of the development of trailing end anchor requirements for the MGS [19]. As part of this research, the same end anchorage used in test no. MGSLS-2 was subjected to a dynamic pull test using the MwRSF heavy bogie vehicle, as shown in Figure 22. In test no. DSAP-2, the end anchorage was loaded until the final BCT post fractured at the base and released the anchor cable, as shown in Figure 23. This was a very similar failure mode to that observed in test no. MGSLS-2. Anchor cable load versus deflection of the foundation tube is shown in Figure 24. The end anchorage in test no. DSAP-2 developed a peak load of 34.6 kips (153.9 kN) at approximately 0.9 in. (23 mm) of deflection prior to failure the final BCT post and release of the anchor cable. The loads observed in test no. DSAP-2 were 25.8% higher than those observed in test no. MGSLS-2 and indicated that the end anchorage that failed during test no. MGSLS-2 had the potential to develop significantly higher end anchor loads prior to failure.

In order to further investigate, a comparison of the anchor load versus time and anchor load versus foundation tube deflection for the available upstream and downstream anchor data from test nos. MGSLS-1, MGSMIN-1, and WIDA-1 were compared with the results from the failed downstream end anchorage in test no. MGSLS-2. The results were divided between upstream and downstream anchor data, and the comparisons are shown in Figure 25 and Figure 26. Review of the upstream end anchor load versus deflection data from the selected tests found that the peak upstream end anchor load was similar to or less than several previous full-scale crash tests, including test nos. MGSMIN-1 and MGSLS-1. This would suggest that the tensile rail loads developed in test no. MGSLS-2 were not excessive as compared to previous MGS barrier tests that did not experience anchor failure. It was also noted that the upstream end anchorage in test no. MGSLS-1 developed a peak load of 34.0 kips (151.2 kN) without anchor failure, which was 23.6% more than the measured peak load in the downstream end anchorage that failed in test no. MGSLS-2. The load versus deflection plot also displayed similar slopes for the four tests. Test nos. MGSLS-2, MGSLS-1, and WIDA-1 had very similar slopes, while test no. MGSMIN-1 displayed increased slope during loading of the end anchorage. This would suggest that the upstream anchors had similar stiffness in the compared tests.

Comparison of the downstream end anchorage load versus deflection data from test nos. MGSLS-1, MGSMIN-1, and MGSLS-2 showed similar trends. The stiffness or slope of the load versus deflection curves were similar for each of the three tests with available data. Additionally, test no. MGSLS-1 developed a peak load in the downstream end anchor of 30.9 kips (137.5 kN) without failure, which was 12.3% higher than the measured peak load in the downstream end anchorage that failed in test no. MGSLS-2.

Analysis and comparison of the end anchorage load and deflection from test no. MGSLS-2 and other comparable tests did not identify a potential source of the end anchorage failure observed in test no. MGSLS-2. The peak load recorded in the failed anchorage did not appear to be excessive when compared with similar full-scale crash tests and did not exceed previous dynamic load testing of similar anchorages. The deflection and stiffness of the failed end anchorage did not suggest any significant departure from previous anchor testing. Finally, no behaviors were noted during loading of the end anchorage that were different from those observed in other end anchorages.

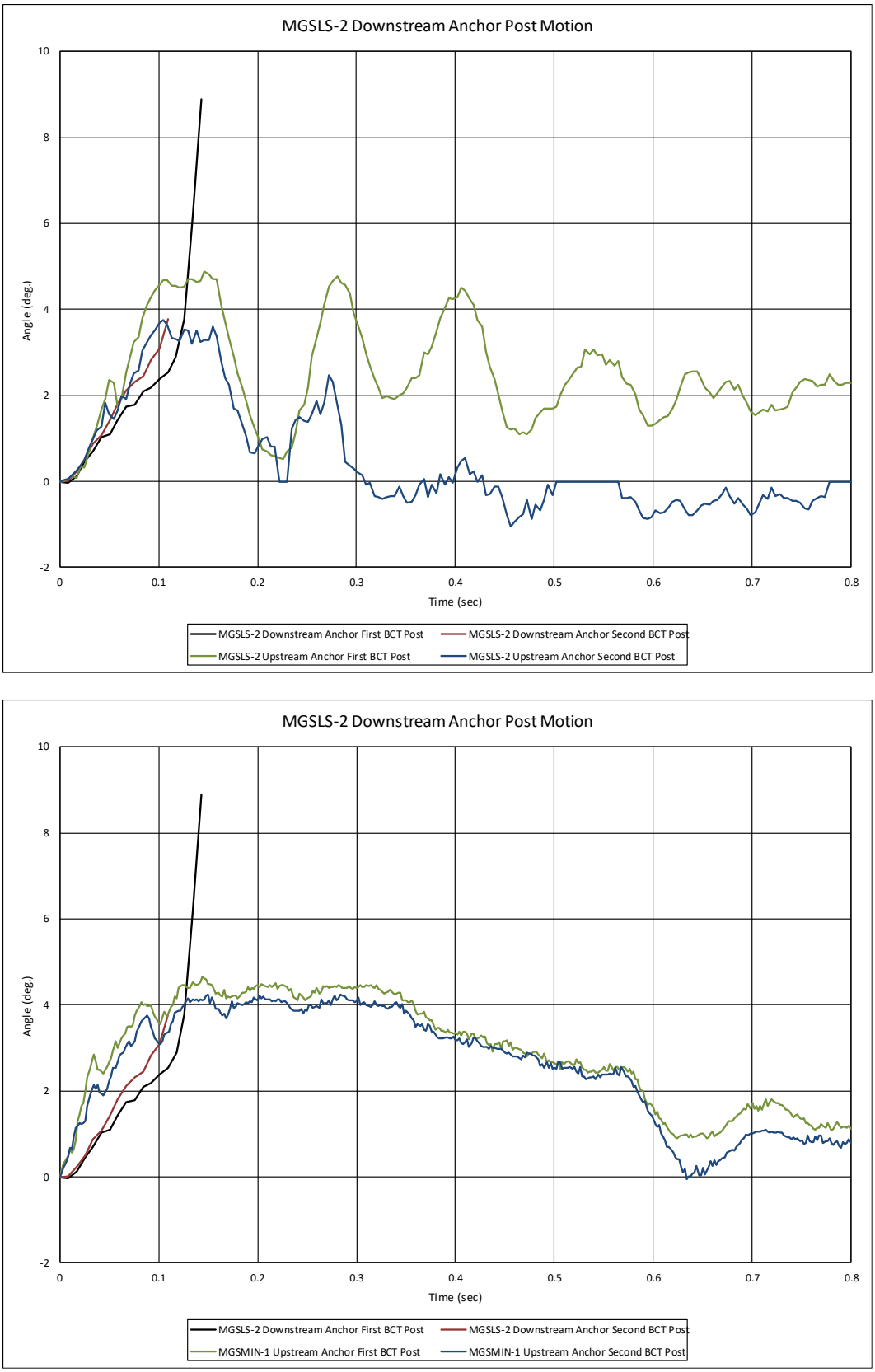

Figure 18. MGSLS-2 Downstream Anchor Post Motion

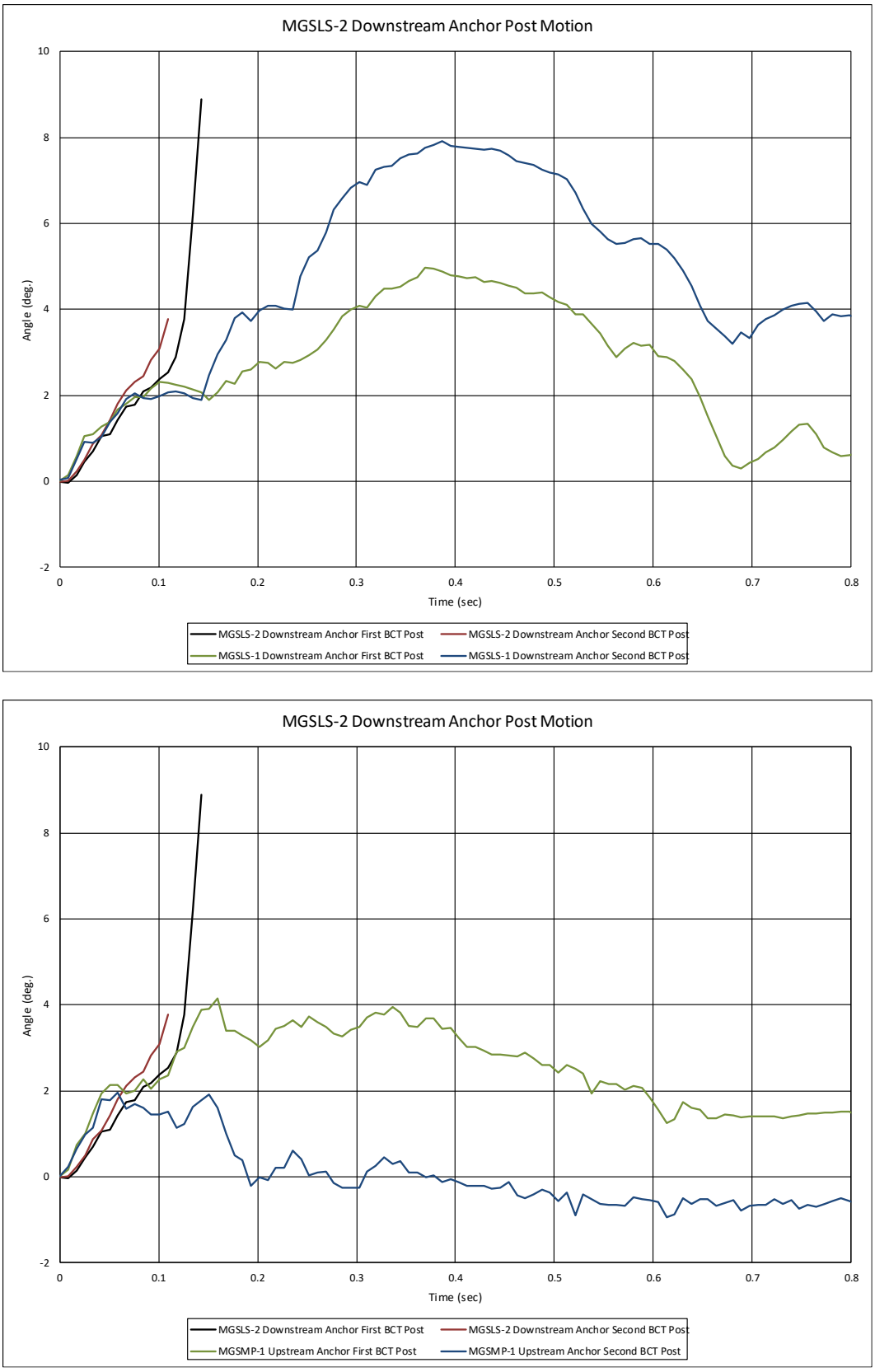

Figure 19. MGSLS-2 Downstream Anchor Post Motion

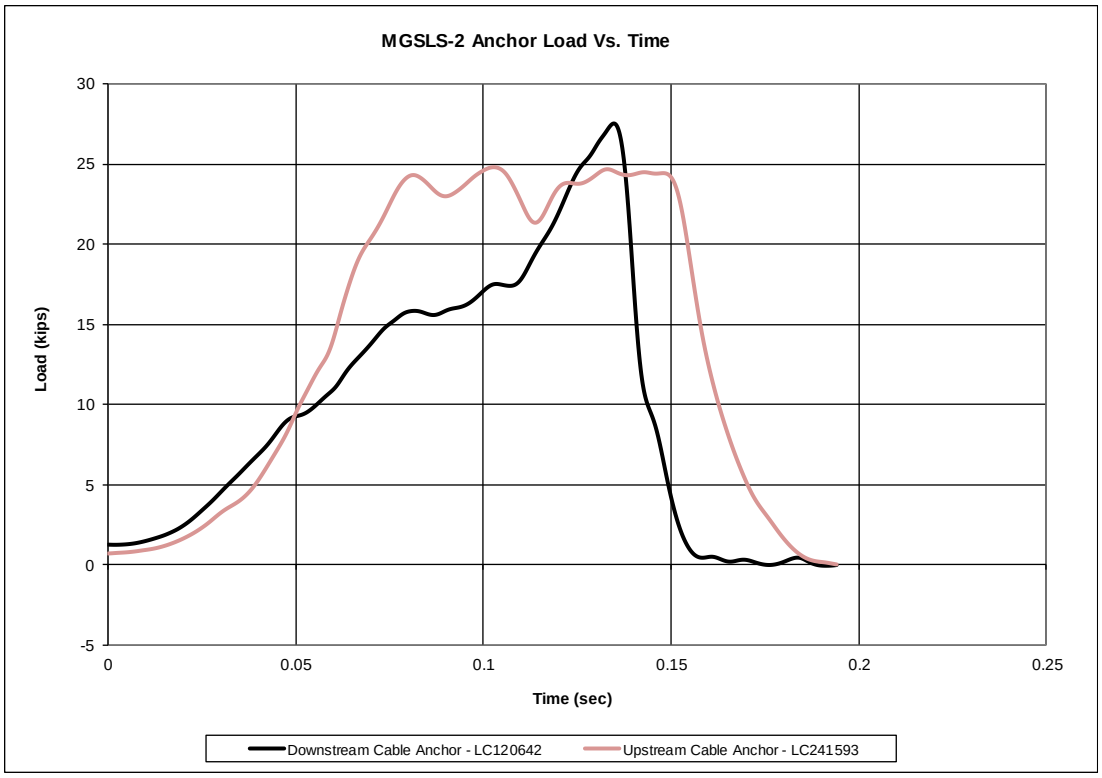

Figure 20. Anchor Load Vs. Time, Test No. MGSLS-2

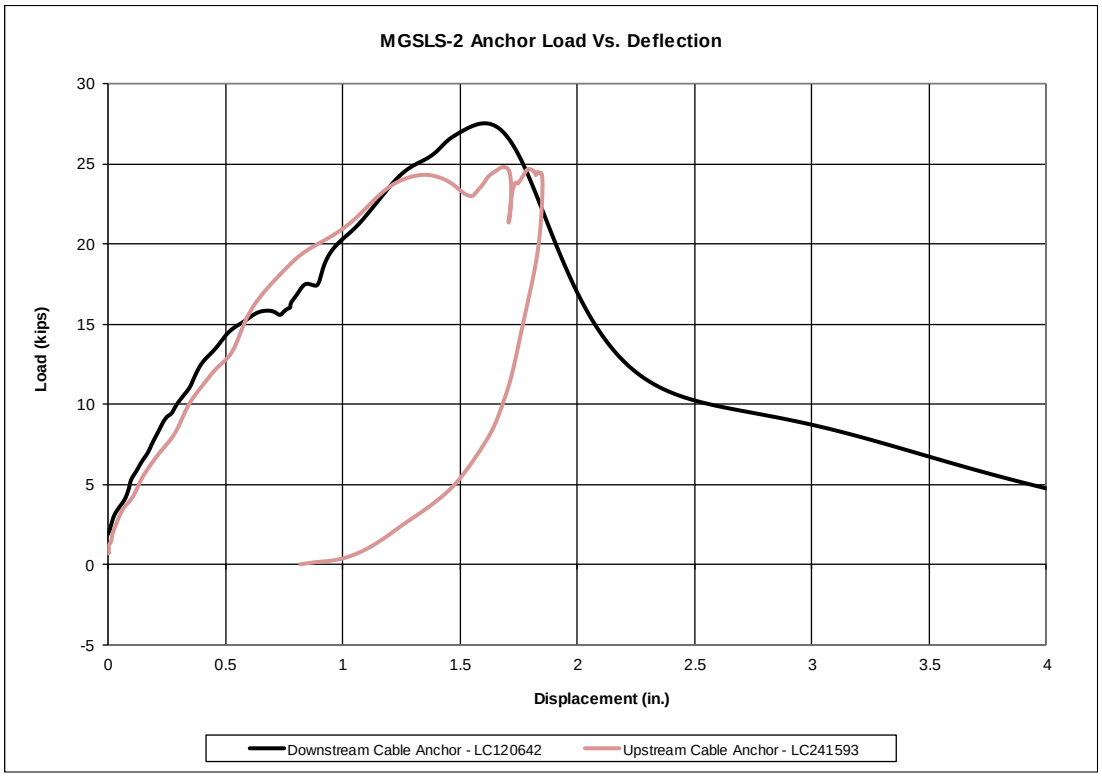

Figure 21. Anchor Load Vs. Deflection, Test No. MGSLS-2

Figure 22. Dynamic End Anchorage Test Setup, Test No. DSAP-2


0.000 sec


0.120 sec


0.080 sec


0.140 sec


0.100 sec


0.200 sec

Figure 23. Time-Sequential Photographs – Front View, Test No. DSAP-2

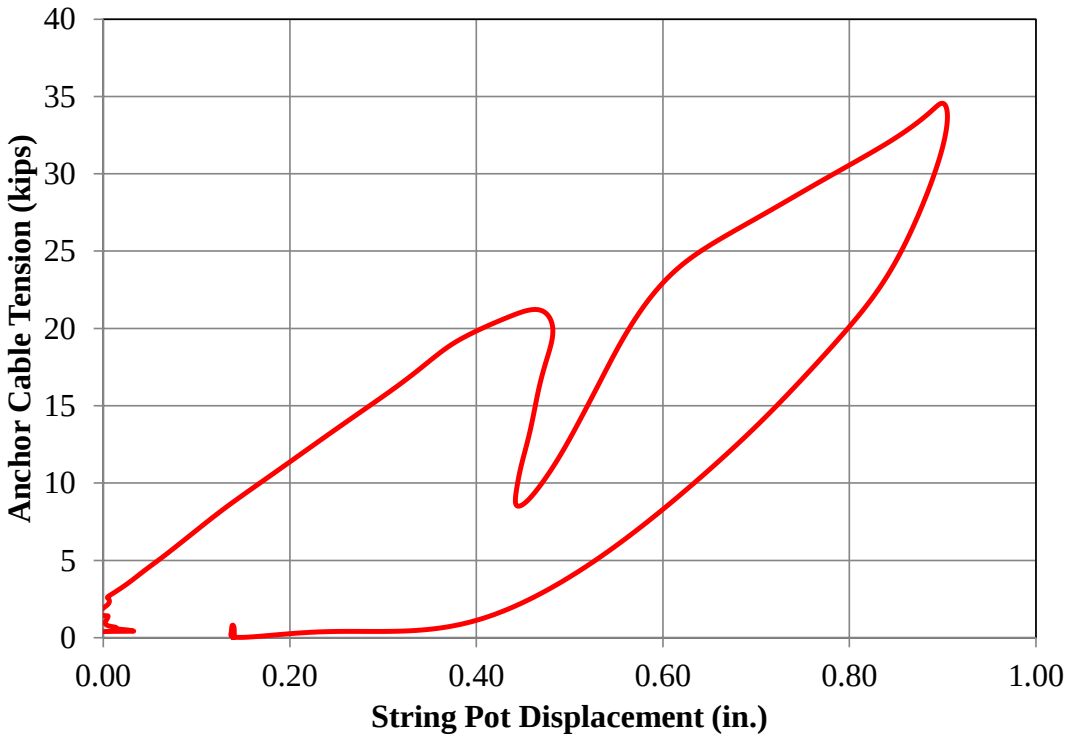

Figure 24. Anchor Cable Load vs. Foundation Tube Displacement, Test No. DSAP-2

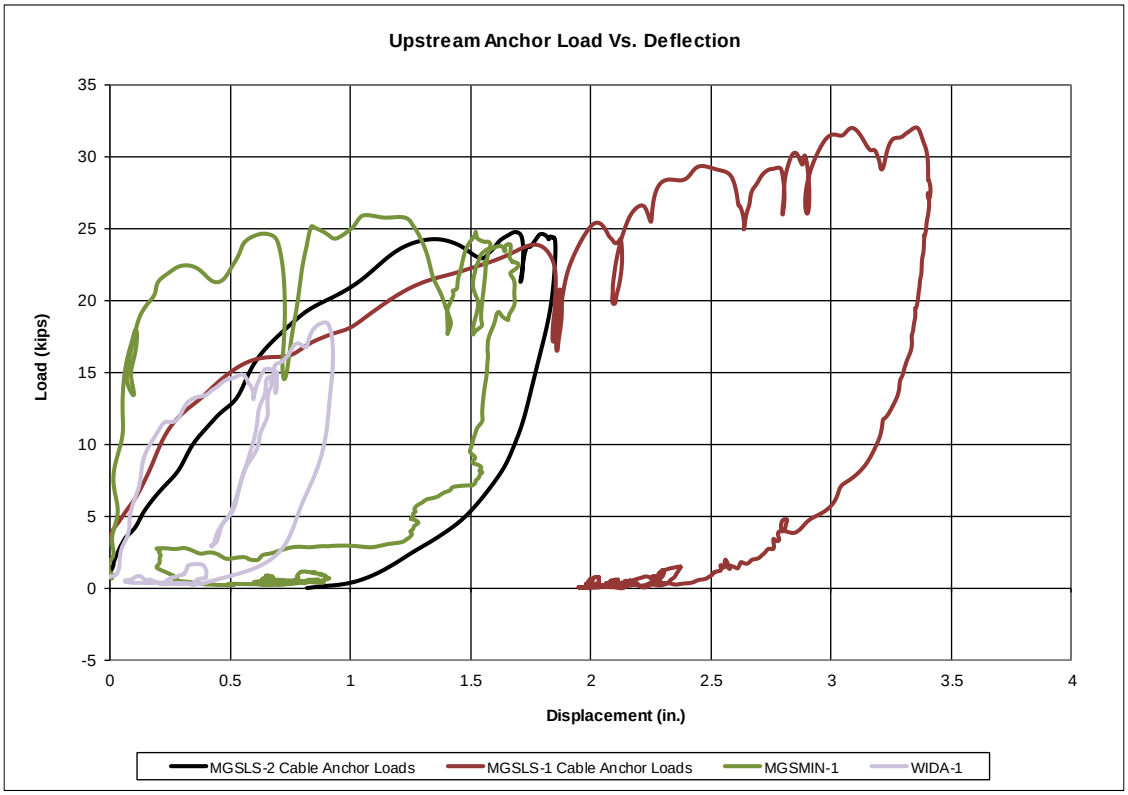

Figure 25. Upstream Anchor Load vs Deflection, Test Nos. MGSLS-2, MGSLS-1, MGSMIN-1, and WIDA-1

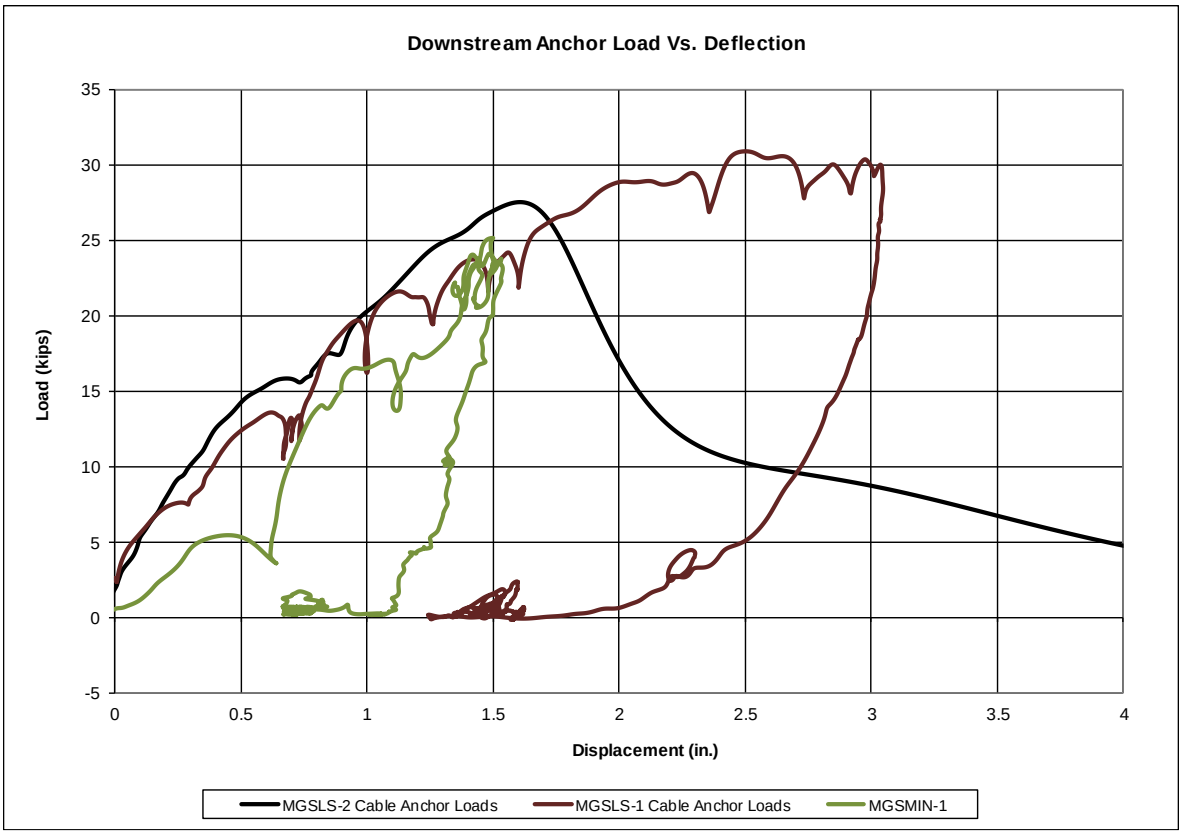

Figure 26. Downstream Anchor Load vs Deflection, Test Nos. MGSLS-2, MGSLS-1, and MGSMIN-1

3.3.2 Location of Vehicle Impact Point

Differences between the vehicle impact point of test no. MGSLS-2 and other comparable tests were reviewed to determine if the vehicle impact point may have contributed to the failure of the downstream end anchorage. The impact point for test no. MGSLS-2 was compared with other similar tests with respect to its proximity to the first post downstream of impact, its proximity to the first rail splice downstream of impact, and the distance to the downstream end anchorage. It was believed that the position of the vehicle impact relative to these critical points may have affected the barrier performance and altered the loading of the end anchorage. Impact points for test no. MGSLS-2 and several comparable tests are shown in Figure 27 and Figure 28. The impact points relative to the first post downstream of impact and the first splice downstream of impact to for test no. MGSLS-2 and comparable tests are shown in Figure 29 and Figure 30, respectively. Finally, the position of the impact points for each test relative to the location of the downstream end anchorage is shown in Figure 31.

Review of the data found that the impact point for test no. MGSLS-2 fell into the mid-range with respect to distance to the first post downstream of impact, which suggested that the impact point with respect to the first impacted post likely had little effect on loading of the end anchorage. However, rail pocketing caused by the impact location relative to a post may have increased anchor loads, as noted previously. Similarly, the distance from the impact point to the first splice downstream for test no. MGSLS-2 fell into the mid-range of the comparable systems. It was noted that in test no. MGSLS-2 the impact was closer to the downstream end anchorage than in previous long span guardrail tests and was closer to the end of the guardrail system than all comparable tests except test nos. WIDA-1 and MGSMIN-1. Test no. LSC-1 was impacted farther from the first post downstream of the unsupported span than test no. MGSLS-2, but no concerns with anchor failure were associated with the former test. Test no. WIDA-1 evaluated an impact near the end of the redirective length of the MGS with a trailing end terminal. In this test, the end anchor failed, but it did not release until the 2270P vehicle had nearly reached the end of the barrier system, and high lateral and longitudinal loads were imparted on the trailing end anchorage. Thus, the failure mode was not similar to the failure under longitudinal loading observed in test no. MGSLS-2. Test no. MGSMIN-1 evaluated a 75-ft (22.9-m) long MGS and impacted 56 ft-3 in. (17.1 m) from the end anchorage. However, the 2270P vehicle was safely redirected and no failure of the end anchorage occurred as a result of the impact closer to the downstream end anchorage. Thus, while the impact point for test no. MGSLS-2 was different as compared to previous tests of the MGS and MGS long span, no evidence was found that suggested the impact point directly contributed to the anchor failure.

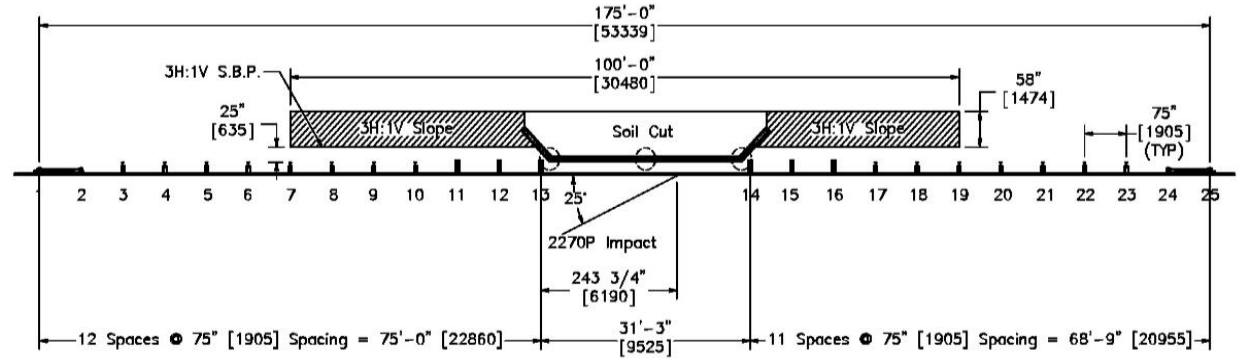

MGSLS-2

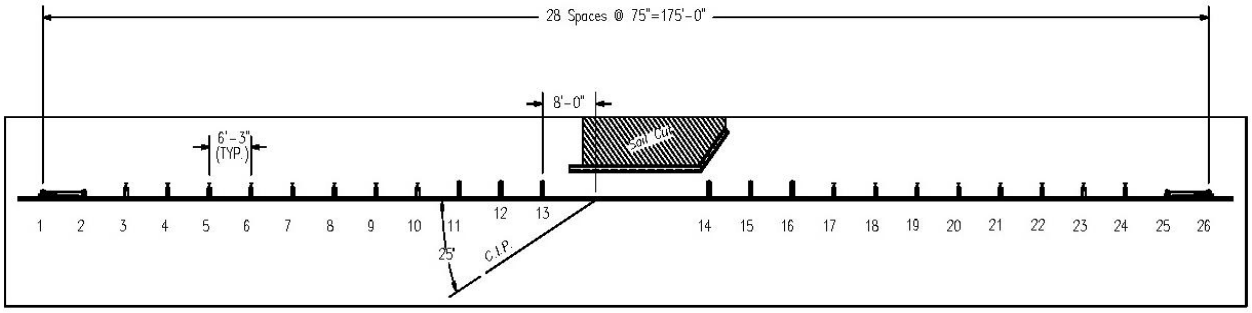

LSC-1

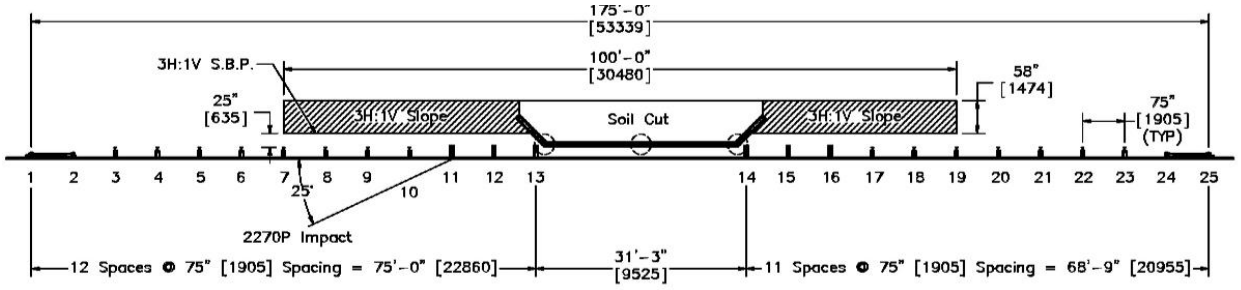

MGSLS-1

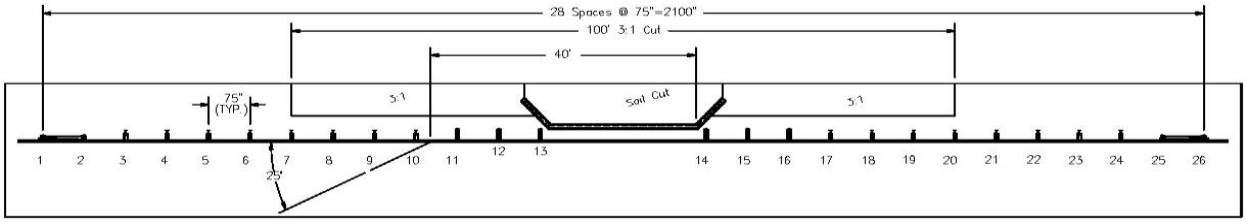

LSC-2

Figure 27. Impact Point for Test Nos. MGSLS-2, LSC-1, MGSLS-1, and LSC-2

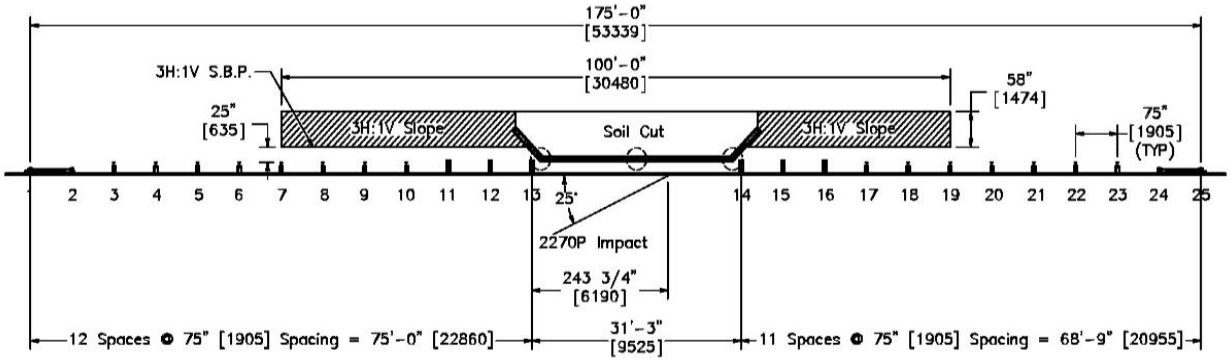

MGSLS-2

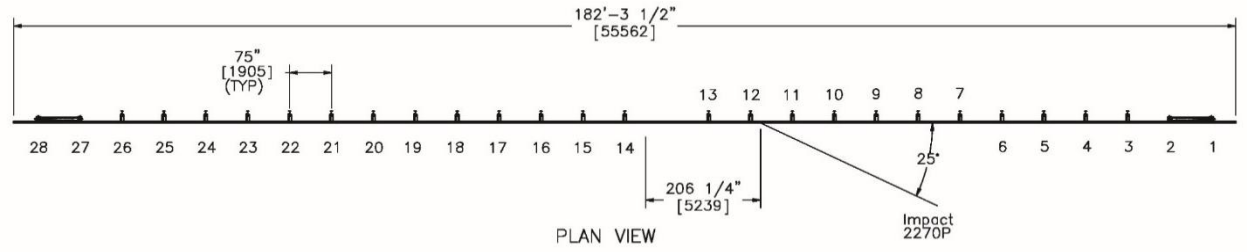

MGSMP-1

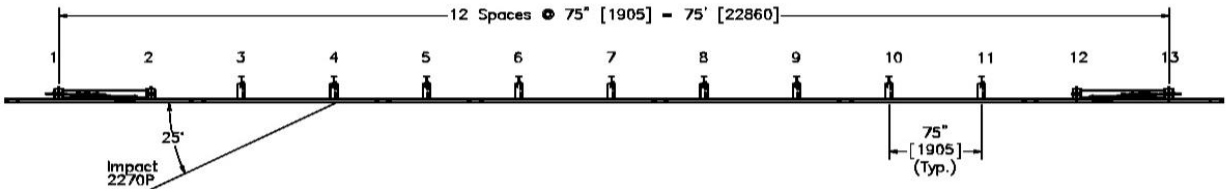

MGSMIN-1

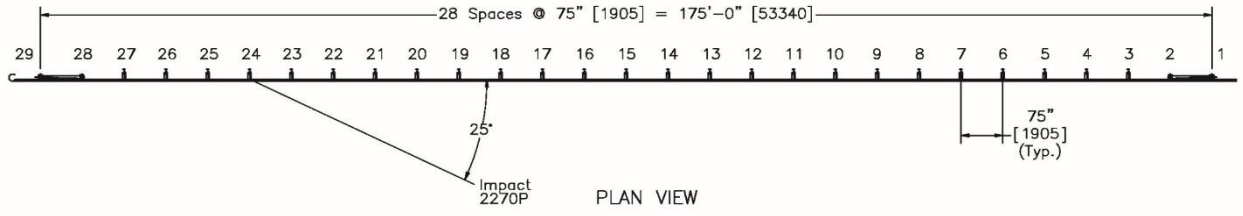

WIDA-2

Figure 28. Impact Point for Test Nos. MGSLS-2, MGSMP-1, MGSMIN-1, and WIDA-2

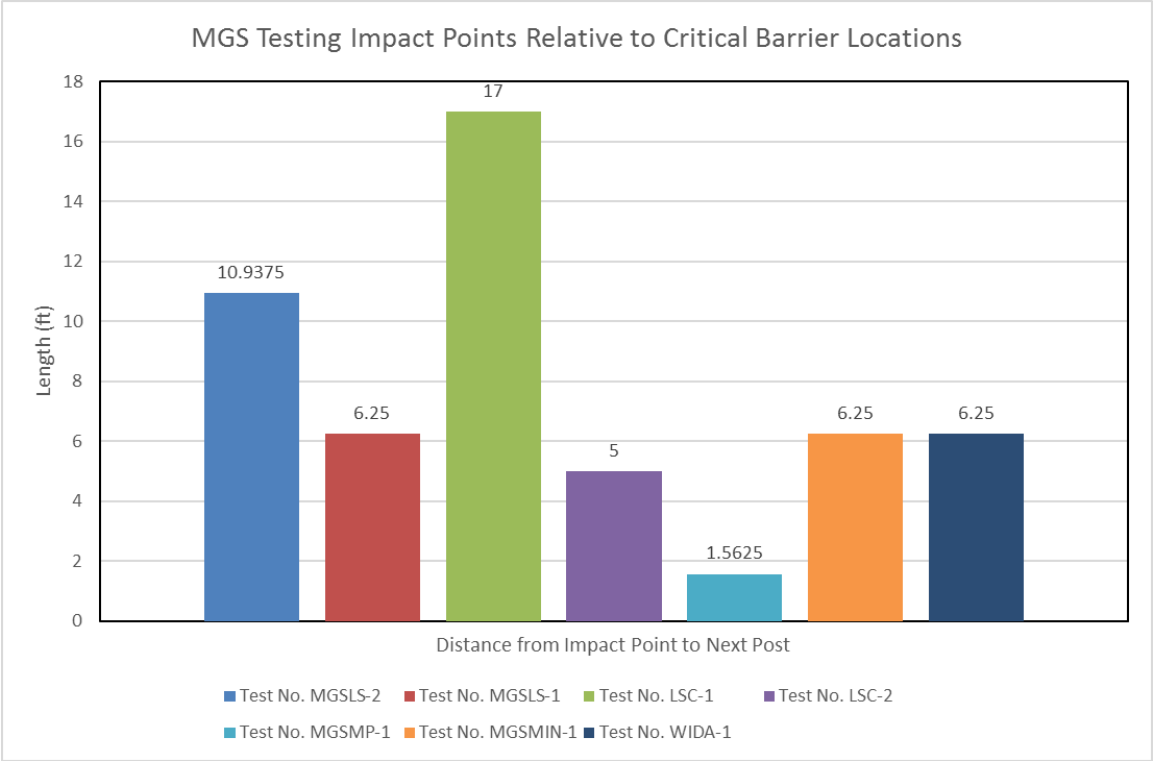

Figure 29. MGS Testing Impact Points Relative to First Post Downstream of Impact

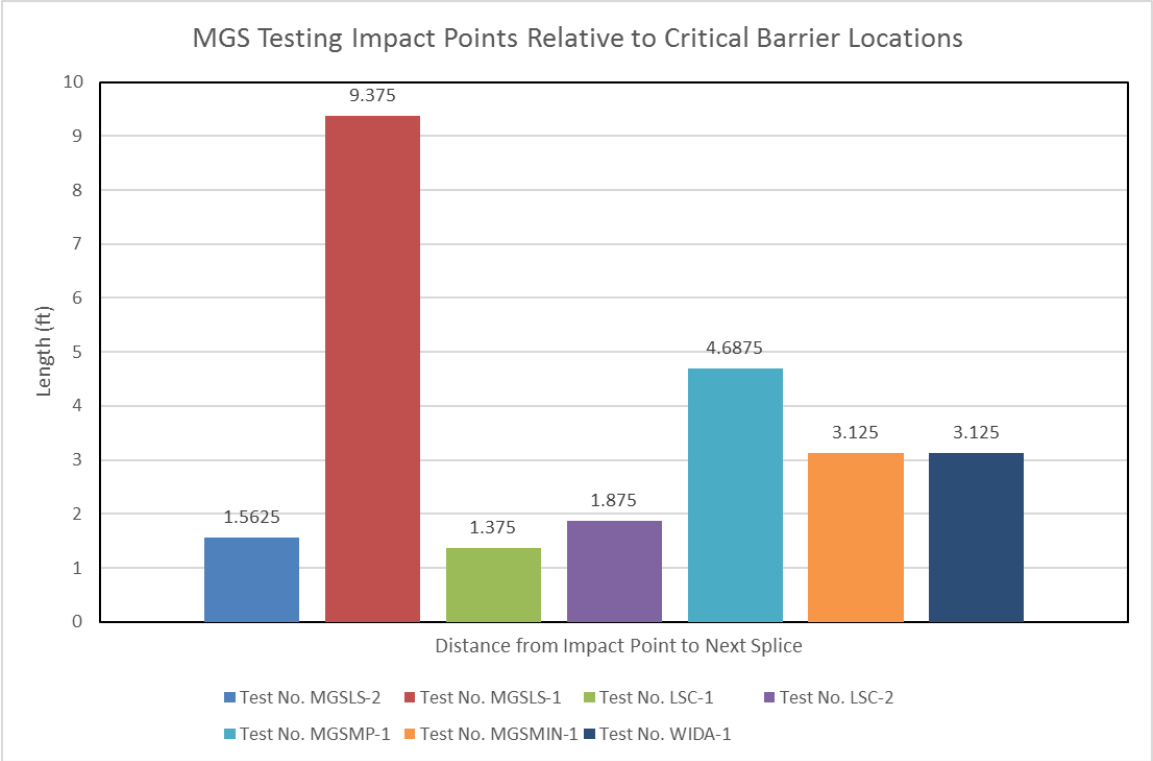

Figure 30. MGS Testing Impact Points Relative to First Splice Downstream of Impact

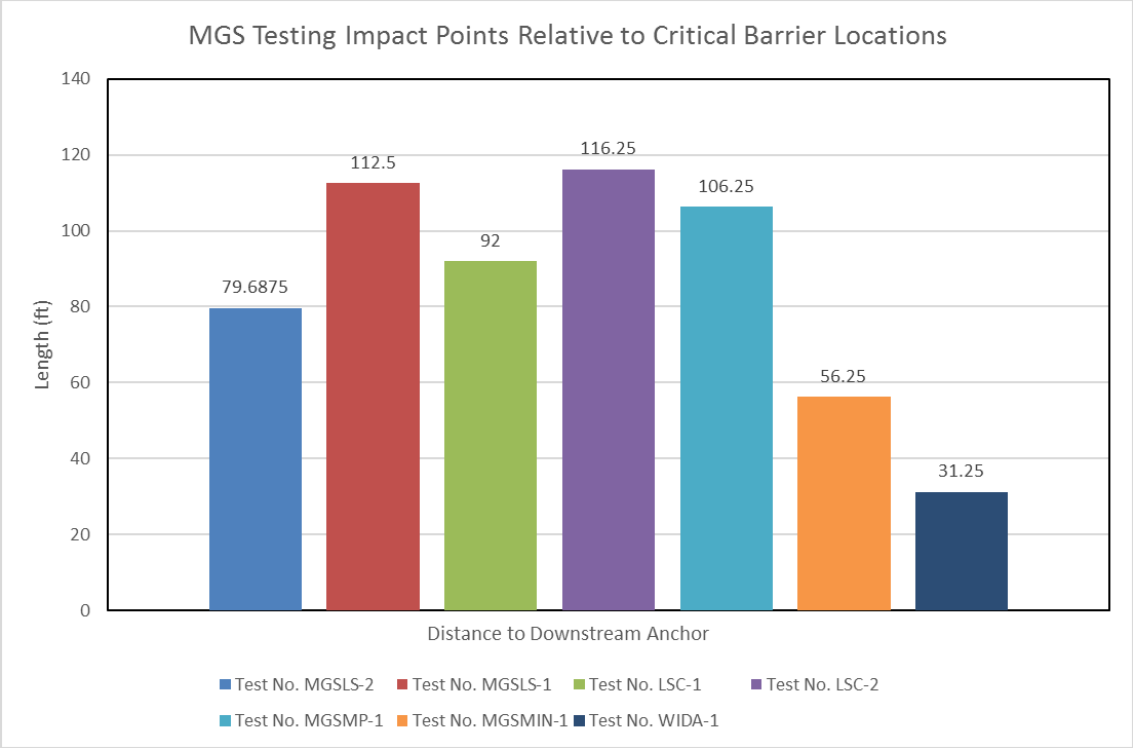

Figure 31. MGS Testing Impact Points Relative to End Anchorage

3.3.3 Breakaway Post Behavior Adjacent to the Unsupported Span

The breakaway post behavior adjacent to the unsupported span was analyzed to determine whether the use of the UBSP when testing the MGS long-span guardrail with an increased span altered the behavior of the system in a manner that may have contributed to the failure of the end anchorage in test no. MGSLS-2. The fracture or disengagement of the UBSPs in test no. MGSLS-2 was compared with the fracture of the CRT posts in previous MGS long span-guardrail test no. LSC-1, which utilized a similar impact point on the unsupported span. Because the vehicle impact points varied for the compared tests, the post disengagement was recorded as a function of the distance from the corner of the impacting vehicle's front bumper relative to each post at the moment it fractured or disengaged, as shown in Figure 32 and Figure 33. This would allow comparison of when the post fractured relative to vehicle position for the two tests. The time of post fracture for each of the posts was also noted.

The comparison of post fracture and disengagement in test nos. MGSLS-2 vs LSC-1 is shown in Table 2. Review of the data found that the UBSPs in test no. MGSLS-2 broke away when the truck was significantly closer to the post as compared to test no. LSC-1. Comparison of post breakaway was most relevant for the first breakaway post downstream of the unsupported span in each test, as anchor failure occurred in test no. MGSLS-2 prior to breakaway of the second and third posts downstream of the unsupported span. The first breakaway post downstream of the unsupported span in test no. MGSLS-2 disengaged when the truck was 18.7 in. (475 mm) closer as compared to the disengagement of the same post in test no. LSC-1. This may indicate that the UBSP provided additional support to the guardrail prior to fracture and may have led to increased barrier stiffness and rail pocketing. Another factor in the delayed disengagement of the UBSP post

may have been that some of the CRT posts in test no. LSC-1 fractured at the second weakening hole in the CRT post below grade, as well as splitting vertically. The UBSP only has a fracture mechanism at ground line and is made of steel. Thus, it cannot replicate a failure of the post below grade or the vertical splitting observed in test no. LSC-1.

Fracture of First UBSP Downstream of Unsupported Span

Fracture of Second UBSP Downstream of Unsupported Span

Fracture of Third UBSP Downstream of Unsupported Span

Figure 32. Longitudinal Distance of Fractured Post Relative to 2270P Bumper Corner, Test no. MGSLS-2

Fracture of First CRT Downstream of Unsupported Span

Fracture of Second CRT Downstream of Unsupported Span

Fracture of Third CRT Downstream of Unsupported Span

Figure 33. Longitudinal Distance of Fractured Post Relative to 2270P Bumper Corner, Test no. LSC-1

Table 2. Breakaway Post Fracture

Post Location	Test No. MGSLS-2		Test No. LSC-1	
	Time at Failure	Post X Distance Relative to Pickup Bumper Corner at Failure (in.)	Time at Failure	Post X Distance Relative to Pickup Bumper Corner at Failure (in.)
First UBSP/CRT Post Downstream of Unsupported Span	0.070	57.4	0.120	76.1
Second UBSP/CRT Post Downstream of Unsupported Span	0.156	42.7	0.150	119.6
Third UBSP/CRT Post Downstream of Unsupported Span	0.278	8	0.168	173.9
*Note: Test no. MGSLS-2 anchor failure occurs between 0.135 and 0.145 sec into event				

3.3.4 Rail Pocketing

Rail pocketing is generally defined as the development of a high angle of the redirective elements of a longitudinal barrier ahead of an impacting vehicle. Rail pocketing angles are a concern due to their potential to affect a system's ability to safely contain and redirect a test vehicle without rupture of the rail components. High rail pocketing angles can lead to increased rail loading, vehicle snag, reduced vehicle capture, and increased longitudinal vehicle decelerations. For test no. MGSLS-2, there was concern that rail pocketing may have occurred that affected the loading of the longitudinal barrier and contributed to the downstream anchor failure. Previous research has indicated that the maximum pocketing angle should fall below 23 degrees, which has previously been associated with degraded barrier performance, including rail rupture [21].

The maximum pocketing angle for test no. MGSLS-2, as well as comparable test nos. MGSLS-1 and MGSMP-1, were calculated from analysis of overhead video. Sequential images of the overhead video from 0.000 sec to 0.140 sec for test nos. MGSLS-2, LSC-1, and MGSMP-1 are shown in Figures 34 through 37, and the calculated pocketing angles are shown in Figure 38. Note that the calculated pocketing angles shown for test no. MGSLS-2 are only relevant up to the point of the downstream end anchor failure at approximately 140 msec after impact. Review of the data found that test no. MGSLS-2 initially had slightly higher pocketing angles than test nos. LSC-1 and MGSMP-1. By 0.040 sec after impact, test no. MGSMP-1 showed a sharp increase in pocketing angle due to the vehicle approaching the first standard line post downstream of the unsupported span created by the omission of a single post. Test no. MGSLS-2 showed a similar increase in pocketing angle as the vehicle approached the first UBSP downstream of the unsupported span. The pocketing angle for test no. MGSLS-2 continued to increase until anchor failure at approximately 0.140 sec after impact. Test no. MGSLS-2 displayed pocketing angles

that were generally greater than those of test no. LSC-1. This was consistent with the earlier disengagement of the CRT posts in test no. LSC-1 noted previously, and may potentially indicate that rail loading was affected by use of the UBSPs. However, anchor load data was not available from test no. LSC-1. The pocketing angles observed for all three tests were less than or very near

Overhead View –Time = 0.000 sec

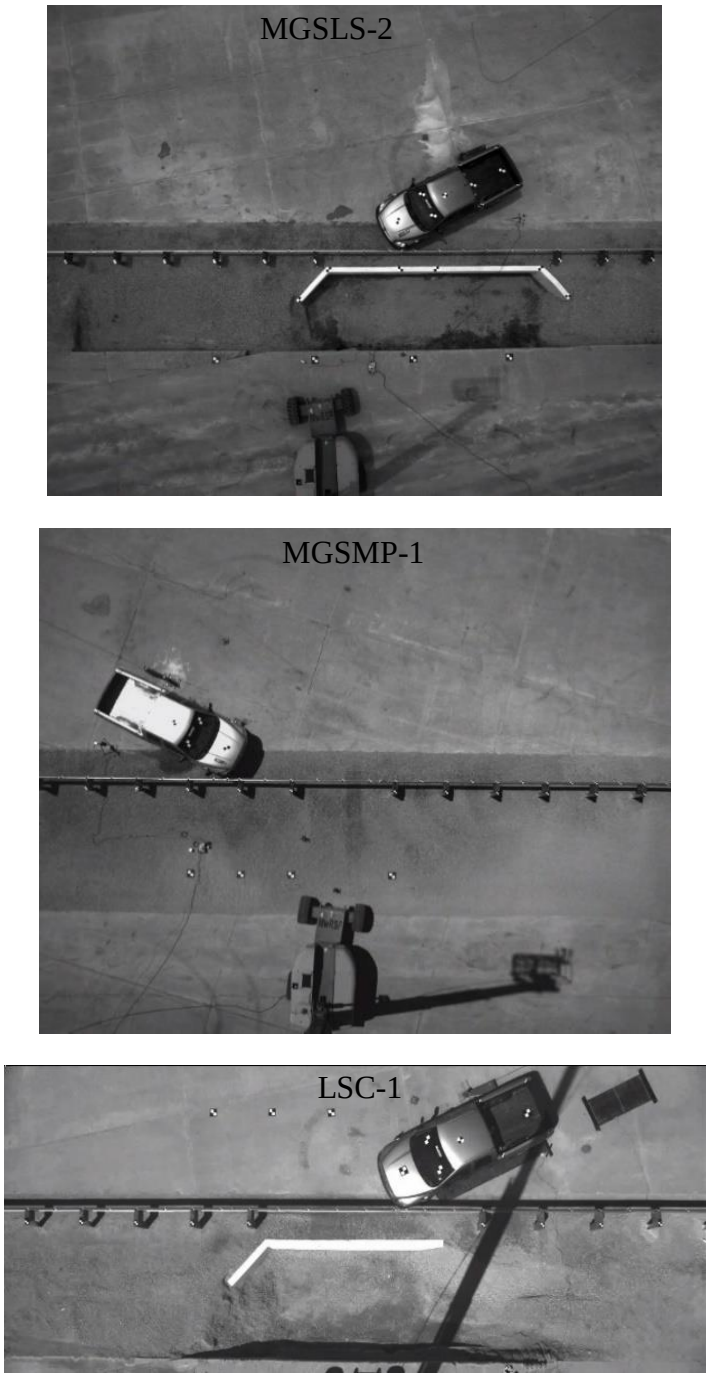

Figure 34. Overhead View at Time = 0.000 sec, Test Nos. MGSLS-2, MGSMP-1, and LSC-1

Overhead View –Time = 0.060 sec

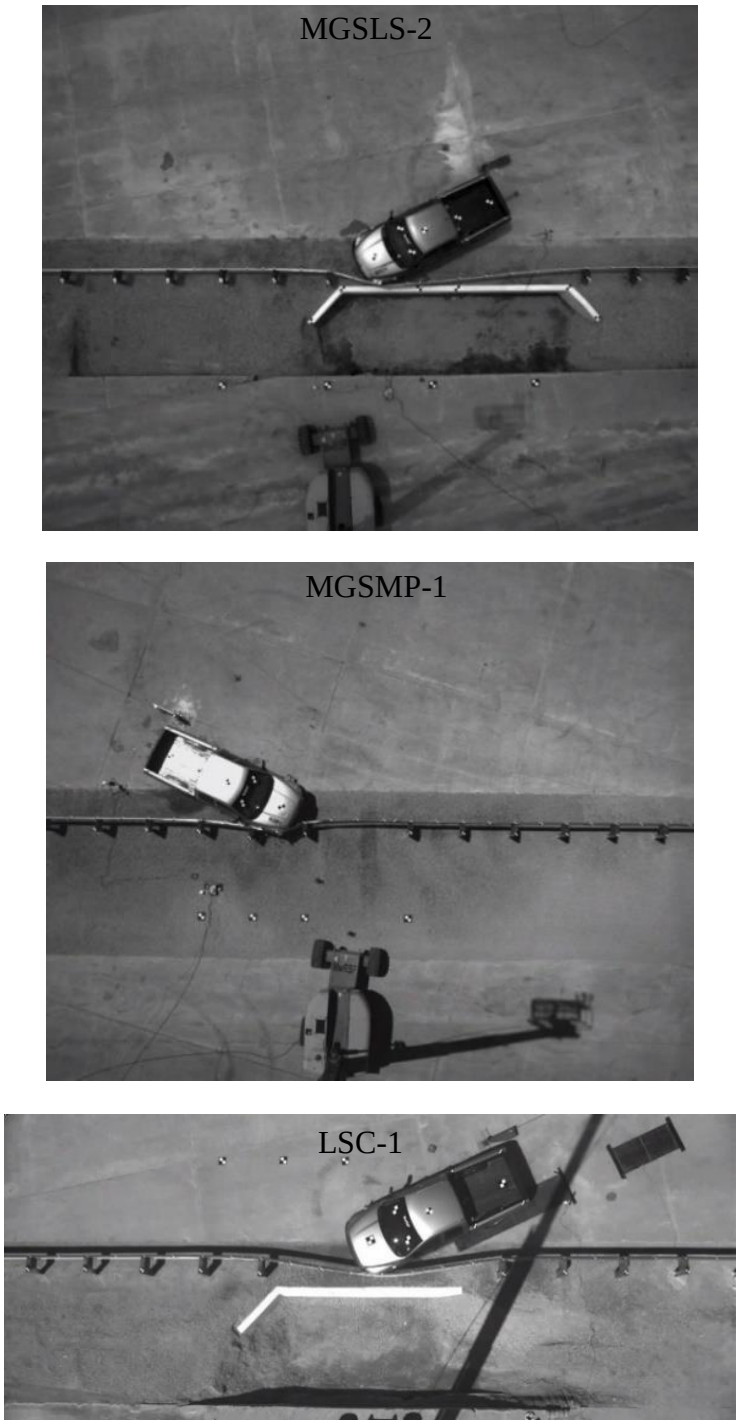

Figure 35. Overhead View at Time = 0.060 sec, Test Nos. MGSLS-2, MGSMP-1, and LSC-1

Overhead View - Time = 0.120 sec

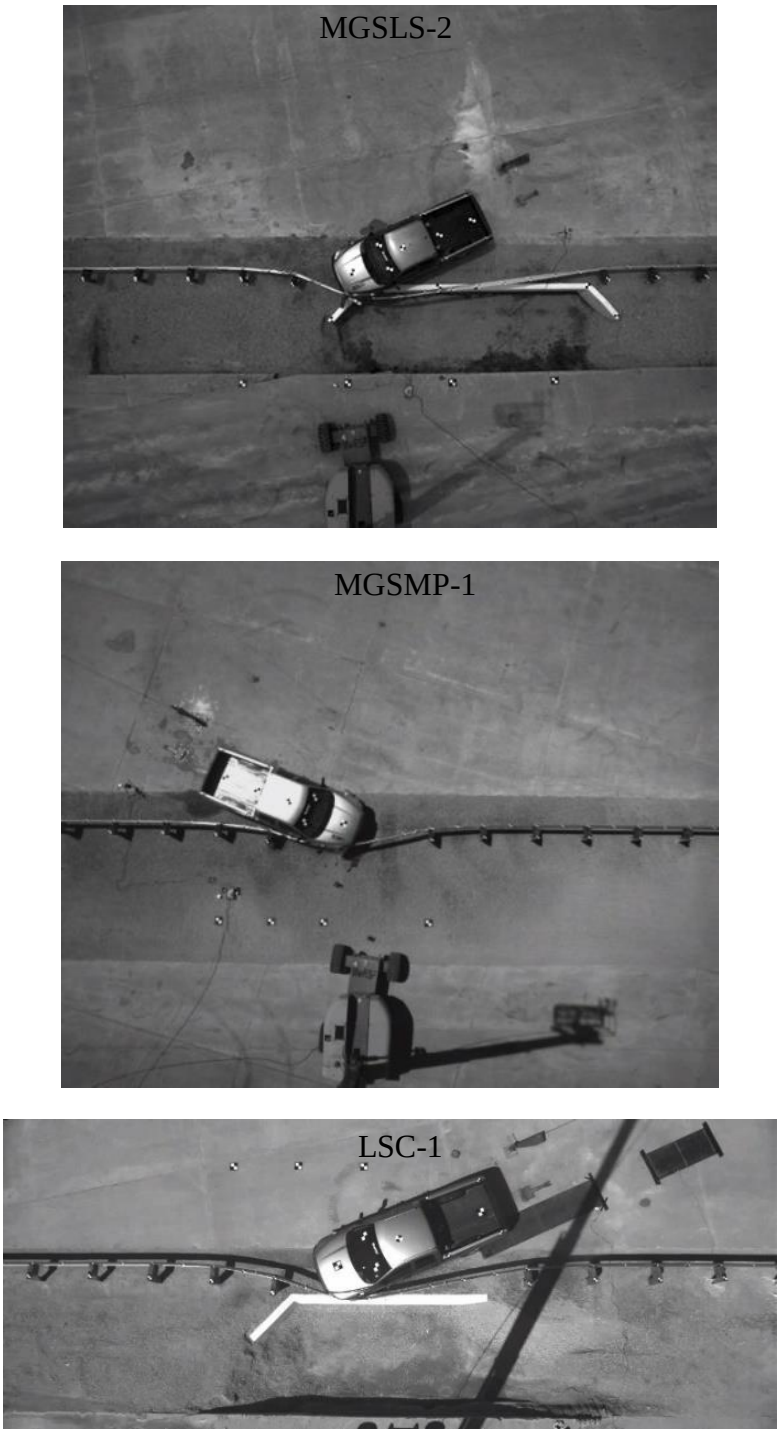

Figure 36. Overhead View at Time = 0.120 sec, Test Nos. MGSLS-2, MGSMP-1, and LSC-1

Overhead View - Time = 0.140 sec

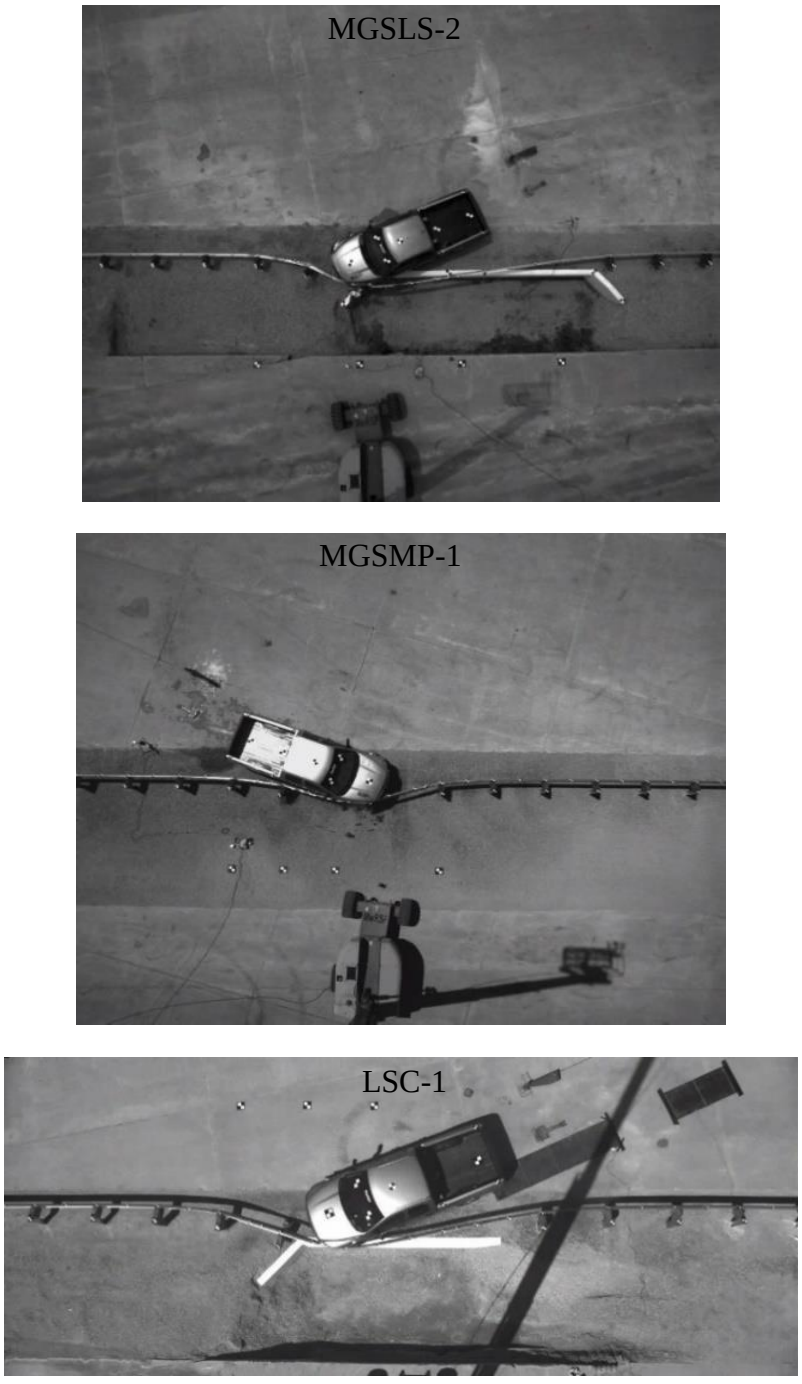

Figure 37. Overhead View at Time = 0.140 sec, Test Nos. MGSLS-2, MGSMP-1, and LSC-1

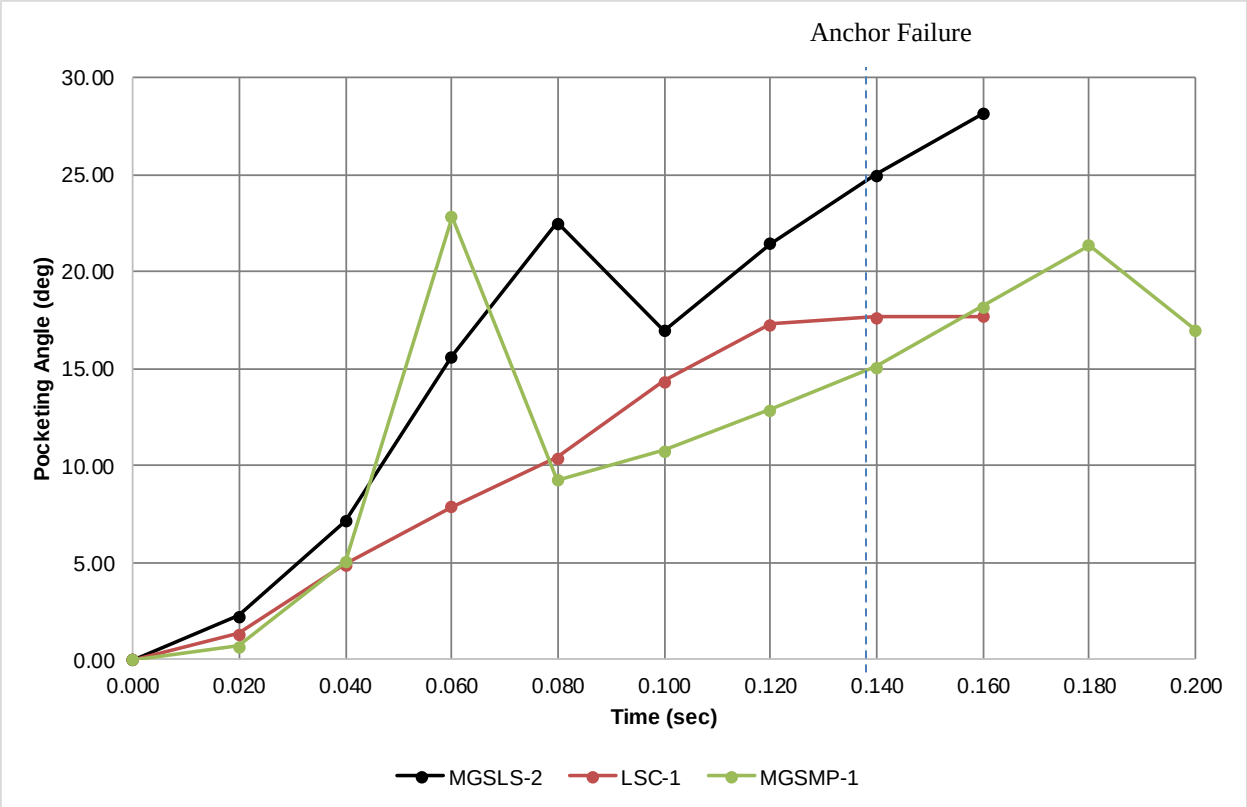

Figure 38. Pocketing Angle Versus Time, Test Nos. MGSLS-2, MGSMP-1, and LSC-1

the threshold of 23 degrees that has previously been deemed acceptable. Additionally, the maximum pocketing angles for test nos. MGSLS-2 and MGSMP-1 were very similar prior to anchor failure, but the end anchor in test no. MGSMP-1 did not fail. The pocketing analysis also noted that some kinking of the rail was observed at the first post downstream of the unsupported span in test no. MGSLS-2 which was not observed in test nos. MGSMP-1 and LSC-1. This may indicate that the UBSP provided additional stiffness prior to fracture and potentially affected rail loading as compared the other tested systems. However, the kinking observed was not sufficient to believe to be a direct cause of the failure of the end anchorage.

Thus, the analysis indicated that the rail pocketing observed in test no. MGSLS-2 was more than observed in previous testing of the MGS long-span guardrail and may have affected rail loading, but the magnitude did not appear to be large enough to indicate a serious concern that would lead the researchers to suspect it as the cause of the downstream end anchorage failure. Additionally, while pocketing of the guardrail was similar to previous testing rail loading may have been affected based on the kinking of the rail prior to anchor failure.

3.3.5 Barrier Defection

Similar to the rail pocketing analysis, a comparison of the dynamic rail deflection was conducted for test nos. MGSLS-2 and LSC-1 in order to determine if the rail deflection indicated potential concerns with respect to the failure of the downstream end anchorage. Test no. LSC-1 was chosen for comparison purposes as it was a similar crash test on the MGS long-span guardrail

with the original unsupported span length. The dynamic rail deflection at various time intervals for test nos. MGSLS-2 and LSC-1 is shown in Figures 39 through 42. Test no. MGSLS-2 displayed higher rail deflections at each time interval as compared to test no. LSC-1. The increased deflection was consistent with the effect of the increased unsupported span length in test no. MGSLS-2 and correlated well with the increased pocketing angles noted previously for test no. MGSLS-2. When combined with increased rail pocketing, the increased rail deflection observed would suggest that the loading of the downstream end anchorage in test no. MGSLS-2 may have been affected by modifications to the barrier as compared to the long-span guardrail evaluated in test no. LSC-1. However, the increased rail deflection and pocketing were not believed to be sufficient to precipitate the failure of the downstream anchorage.

3.3.1 Soil Strength

Variation in the soil strength between crash tests was another potential factor that may have contributed to the failure of the downstream end anchorage in test no. MGSLS-2. Increased soil strength could have affected the loading of the downstream end anchorage by increasing the stiffness of the anchorage and reducing the amount of energy absorbed as the anchorage was loaded. Under the MASH test criteria, static soil tests are performed prior to all full-scale crash tests for comparison with a known baseline soil material to ensure that soil strength is above a minimum value. The static soil test data from test no. MGSLS-2 and other comparable tests were reviewed to investigate potential soil strength differences.

A comparison of the force versus deflection data from test nos. MGSLS-2, MGSLS-1, MGSMIN-1, and MGSMP-1 is shown in Figure 43. The data showed that the peak load developed in the static soil test for test no. MGSLS-2 was similar to that of previous tests. The initial slope or stiffness of the soil response was similar as well. The general shape of the curves shown do differ from test to test, but all the soil tests reviewed were acceptable under the MASH soil requirements for full-scale crash testing. Based on these results, the soil response from test no. MGSLS-2 would not have been expected to produce more severe loading of the end anchorage. This conclusion would be consistent with the anchor load comparison, which indicated that the loading of the end anchor was consistent with previous tests of similar anchorages.

Static soil tests from the original full-scale crash testing of the MGS long-span guardrail, test nos. LSC-1 and LSC-2, were not available for comparison. These tests were conducted during the development of the MASH criteria and prior to the development of the static soil testing procedure. While there may have been differences in the stiffness and post -soil interaction forces when comparing the original and increased span length MGS long-span guardrail testing, it was not possible to quantify potential differences in the soil behavior between those systems.

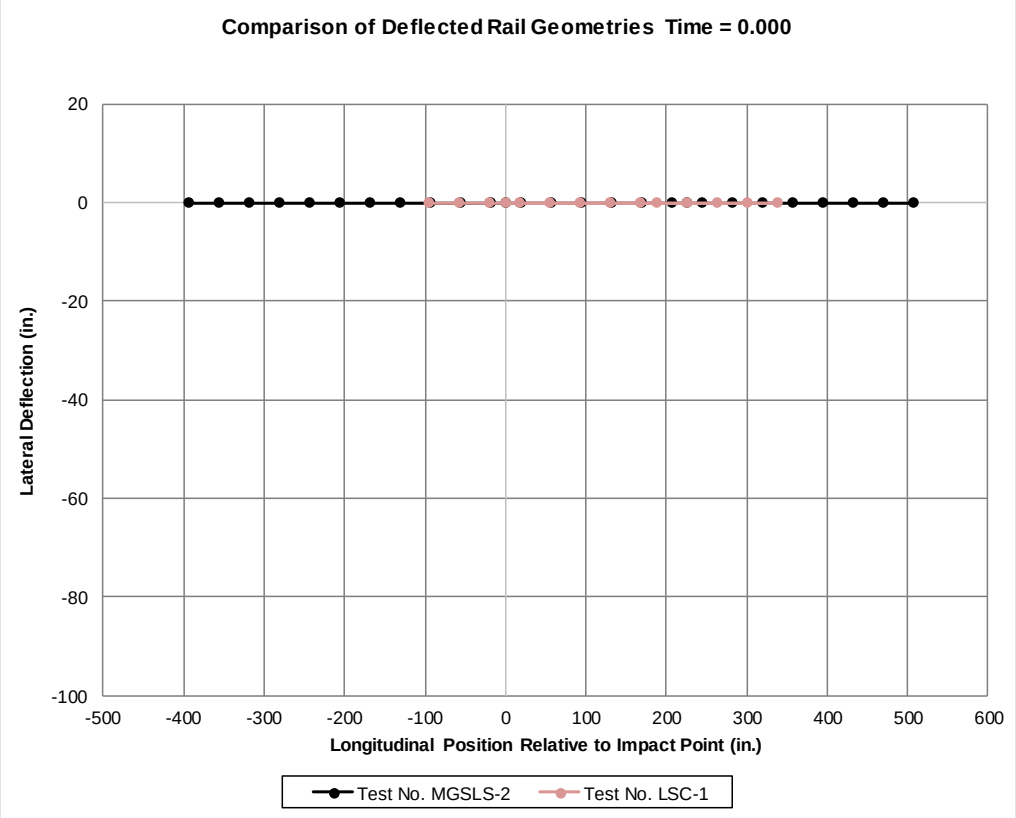

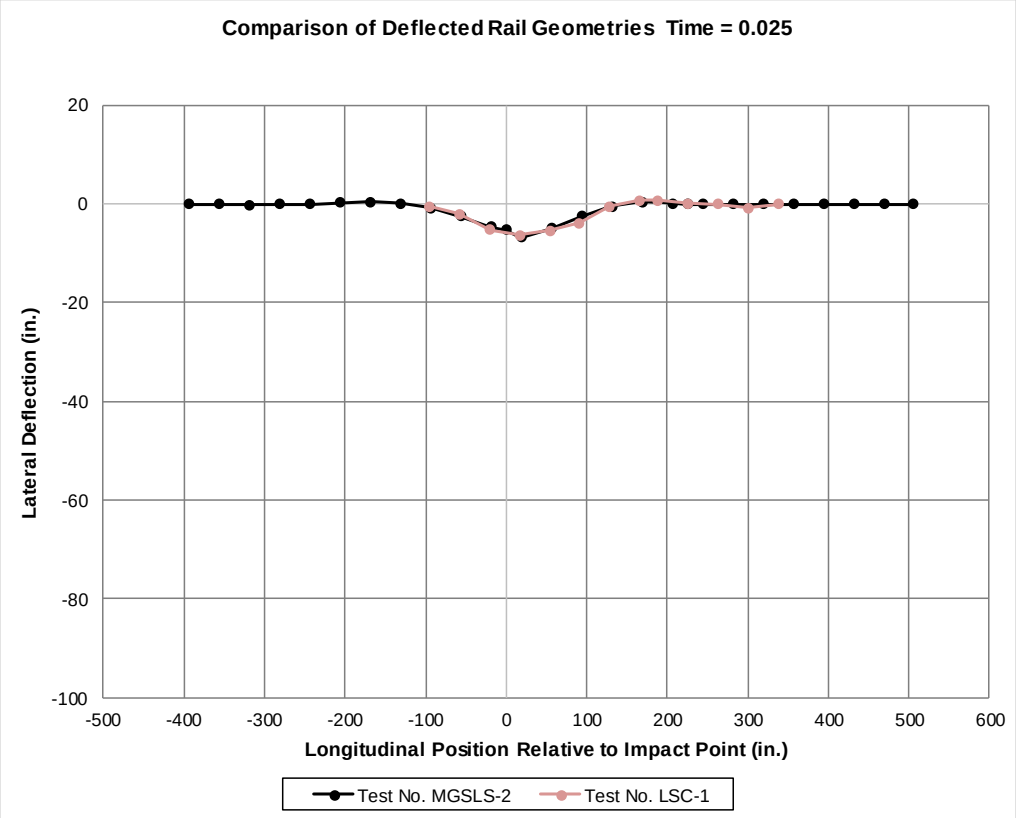

Figure 39. Comparison of Deflected Rail Geometries

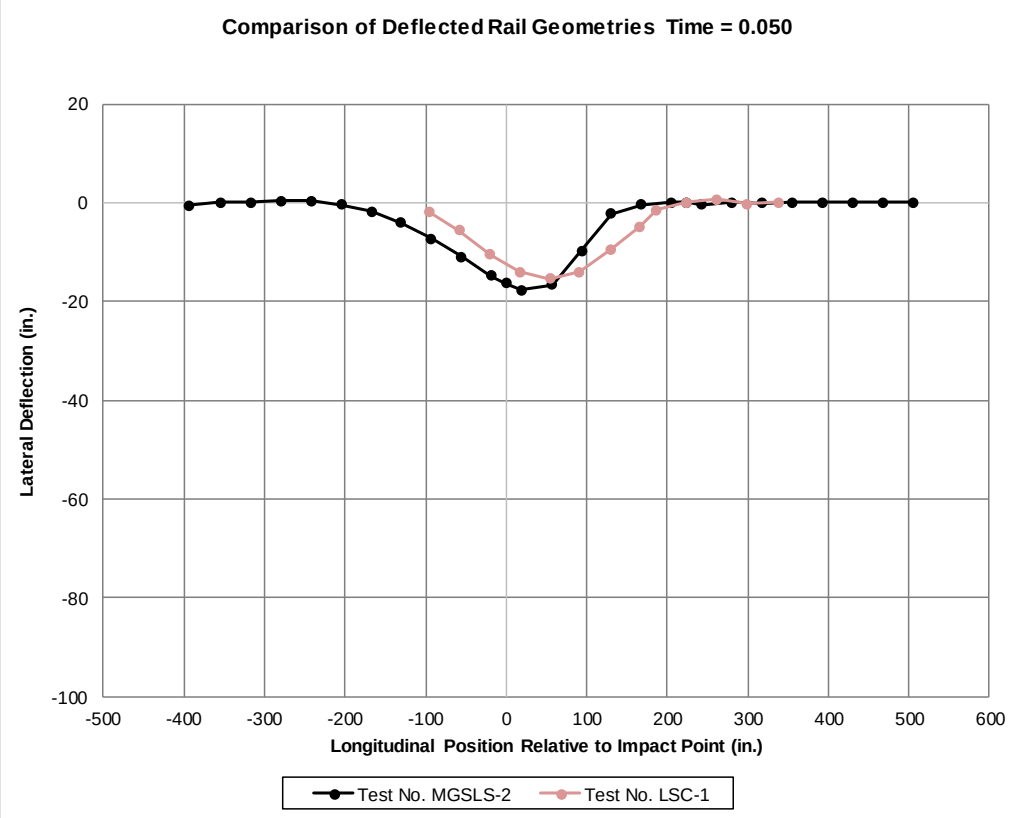

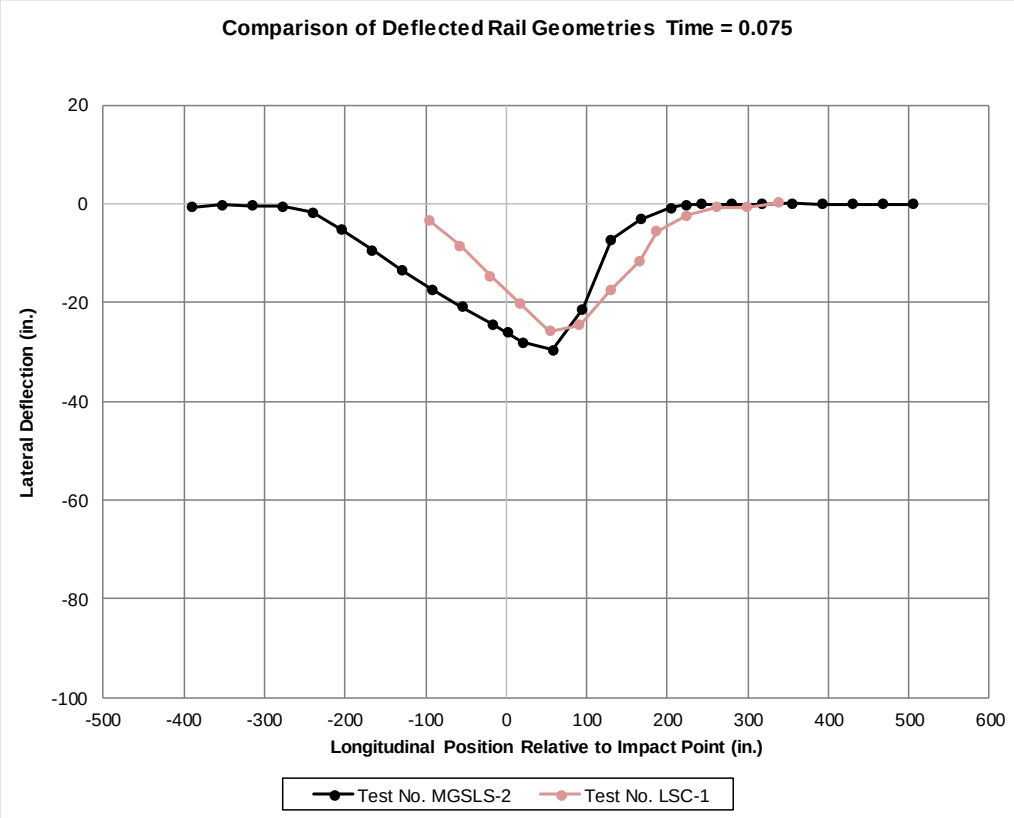

Figure 40. Comparison of Deflected Rail Geometries

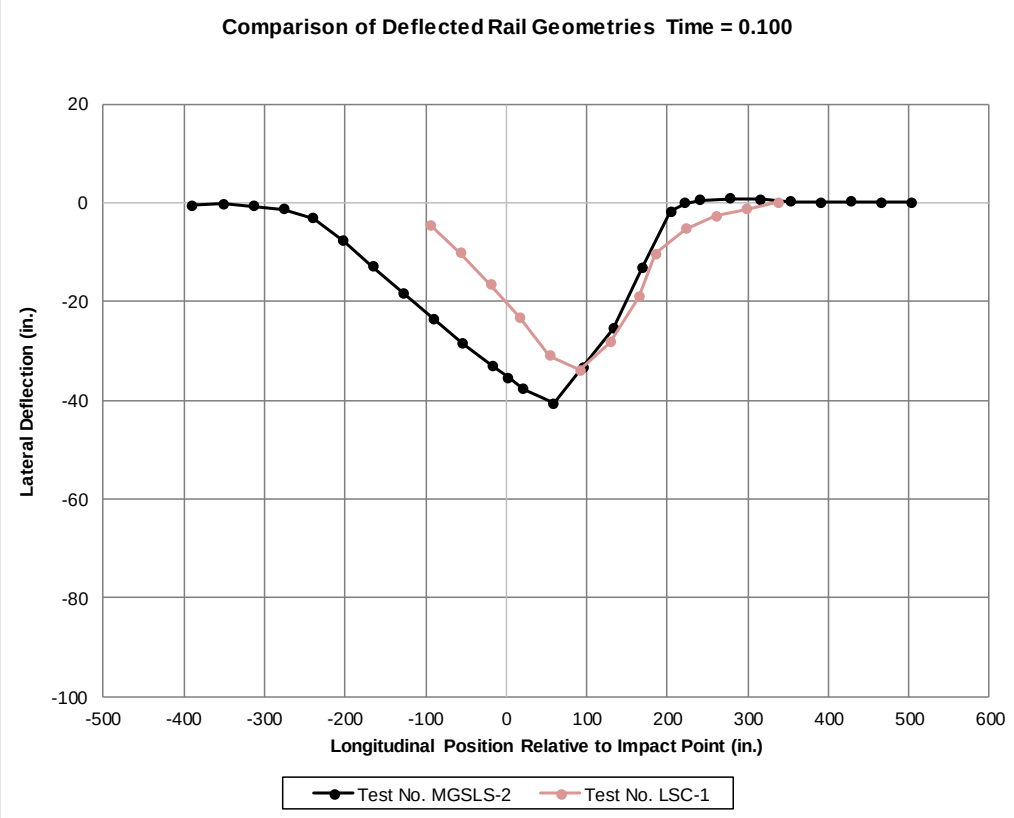

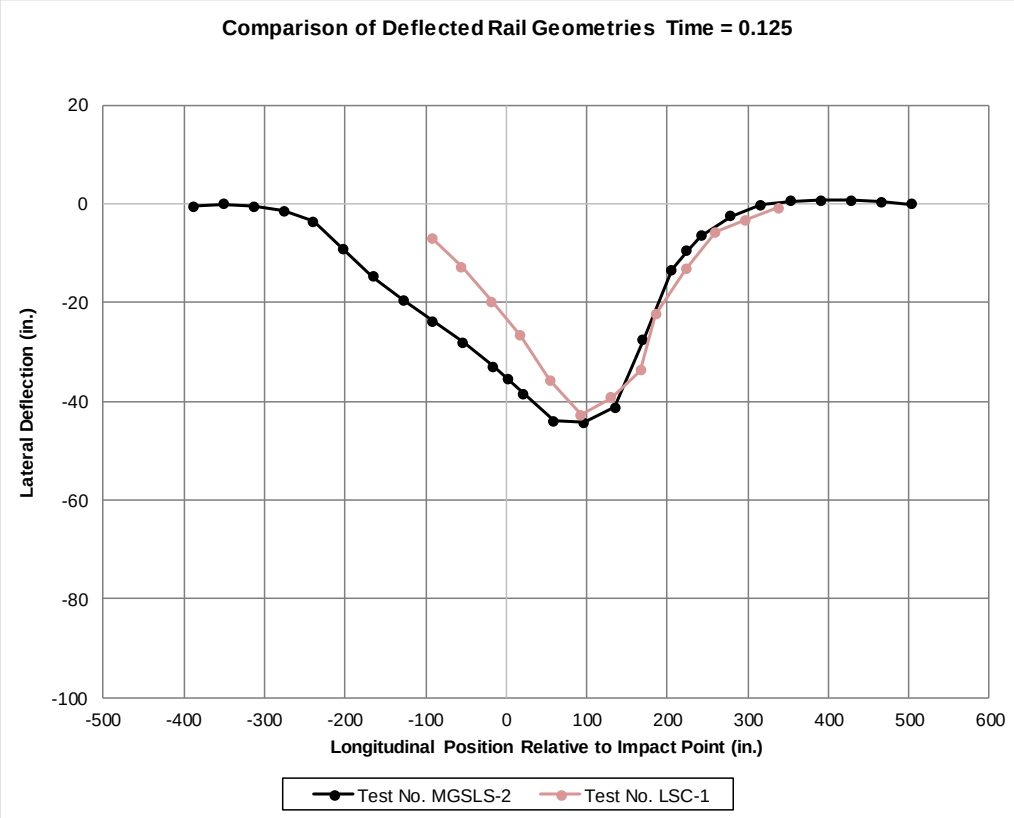

Figure 41. Comparison of Deflected Rail Geometries

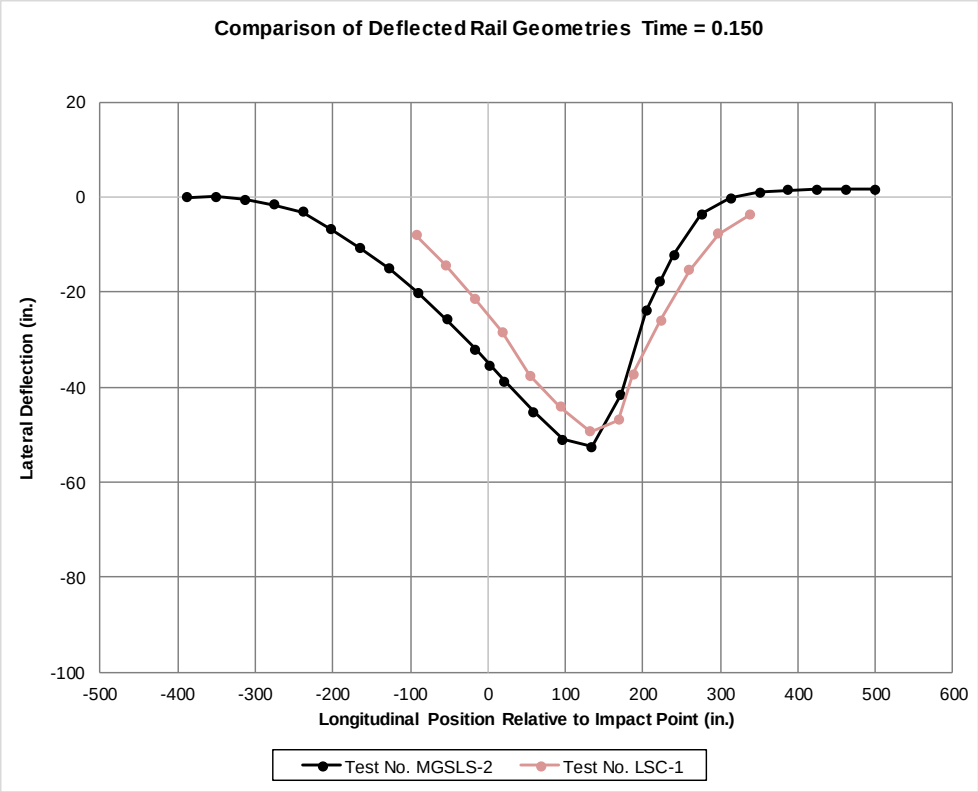

Figure 42. Comparison of Deflected Rail Geometries

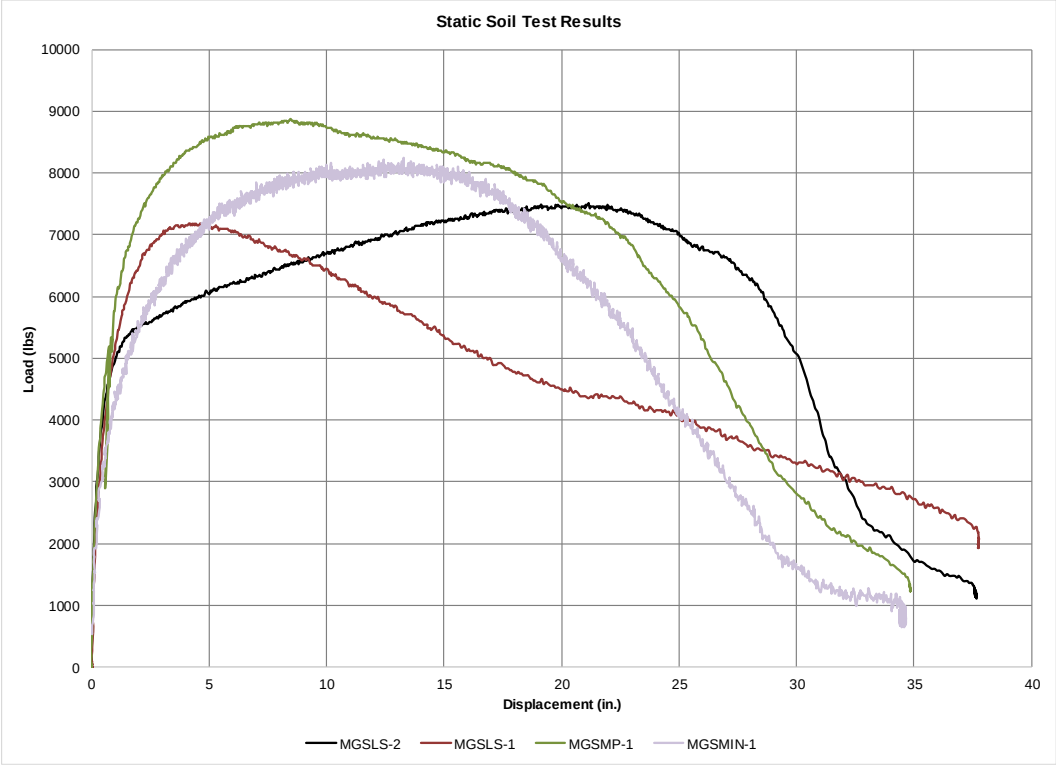

Figure 43. Static Soil Test Comparisons

3.3.2 Wood Variability

Another potential factor that could have affected the failure of the downstream end anchorage in test no. MGSLS-2 was the inherent variability of the southern yellow pine (SYP) BCT posts used in the anchorage. The strength of SYP can vary for several reasons, including natural variations in density, the presence of latewood and earlywood growth rings, and defects such as knots, checks, and shakes. Moisture content and other factors may play a role as well. Figure 44 shows the variability in tension and compression of SYP clear wood at 12% moisture content. The plots show that even clear wood has strengths that vary 50% or more from the median.

The variation of the timber posts used in the end anchorages has affected anchor capacity in previous testing. During the development of a simplified steel post approach guardrail transition for the MGS, an initial crash test, test no. MWTSP-1, was performed according to test designation no. 3-21 of MASH with a ½–ton Quad Cab pickup truck [22]. During the test, the upstream BCT wood anchor posts failed prematurely, causing a loss of tension in the rail which allowed the rail to pocket excessively. As a result, the longitudinal occupant ridedown decelerations exceeded the recommended safety limits established by MASH. Upon inspection, it was determined that a knot located in the critical section of the first BCT wood anchor post led to the premature post failure.

In order to minimize the effect of wood variability observed in test no. MWTSP-1, MwRSF specified that the BCT posts used in full-scale crash tests be Grade No. 1 or better SYP with no knots 18 in. (457 mm) above or below the hole at ground line. In test no. MGSLS-2, similar criteria were used, and review of the fractured posts in the downstream end anchorage found no flaws in critical region of BCT posts. Additionally, the post geometry and system details were consistent with the CAD details and previously tested anchorages. While examination of the fractured posts did not indicate any issues that would have affected the strength and capacity of the end anchorage, the variability of wood strength still may have affected the capacity of the end anchorage.

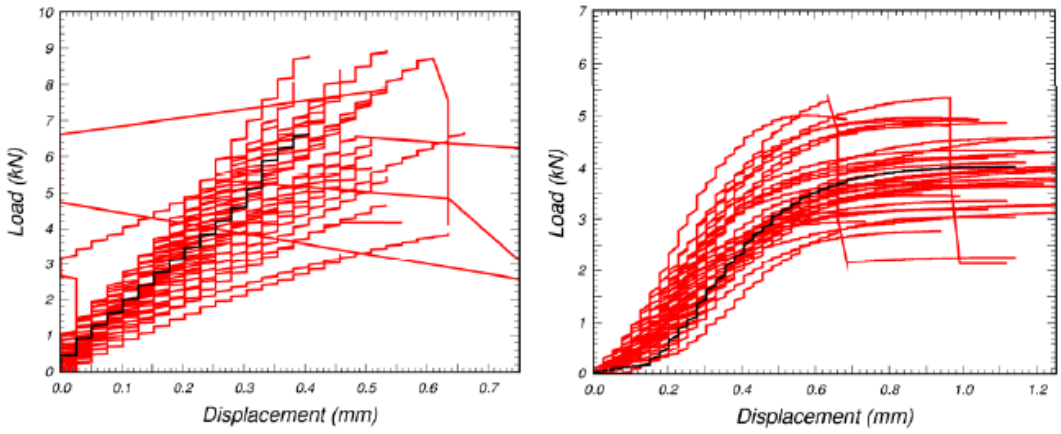

(a) (b)

Figure 44. Southern Yellow Pine (a) Tension Parallel and (b) Compression Perpendicular

3.3.3 Vehicle trajectory

Vehicle trajectory data was reviewed for test no. MGSLS-2 and other comparable tests to determine if the motion of the impacting 2270P vehicle in the failed test provided insight into the

failure of the downstream end anchorage. Trajectory data for test nos. MGSLS-1, LSC-1, LSC-2, and MGSMP-1 were used for comparison purposes. The comparisons were focused on the first 0.150 sec after impact due to failure of the end anchorage in test no. MGSLS-2 at approximately 0.140 sec.

Review of the vehicle roll and pitch data from these five tests showed little to no difference through the first 0.150 sec after impact. All of the vehicles remained very stable with little to no roll or pitch early in the impact. Comparison of the vehicle yaw angles for all five tests is shown in Figure 45. Vehicle roll and pitch was minimal and showed little to no difference prior to anchor failure. The yaw data showed that test no. MGSLS-2 redirected the impacting vehicle more slowly than all tests except test no. LSC-1. The slower yaw rate for these two tests correlated with tests that impacted within the unsupported span of the long-span guardrail. The lack of lateral support of the rail led to lower redirective forces and slower vehicle yaw. While the yaw angle data denoted a different system response for those tests, neither the yaw data nor the vehicle roll and pitch indicated any potential effect on end anchorage loading or failure.

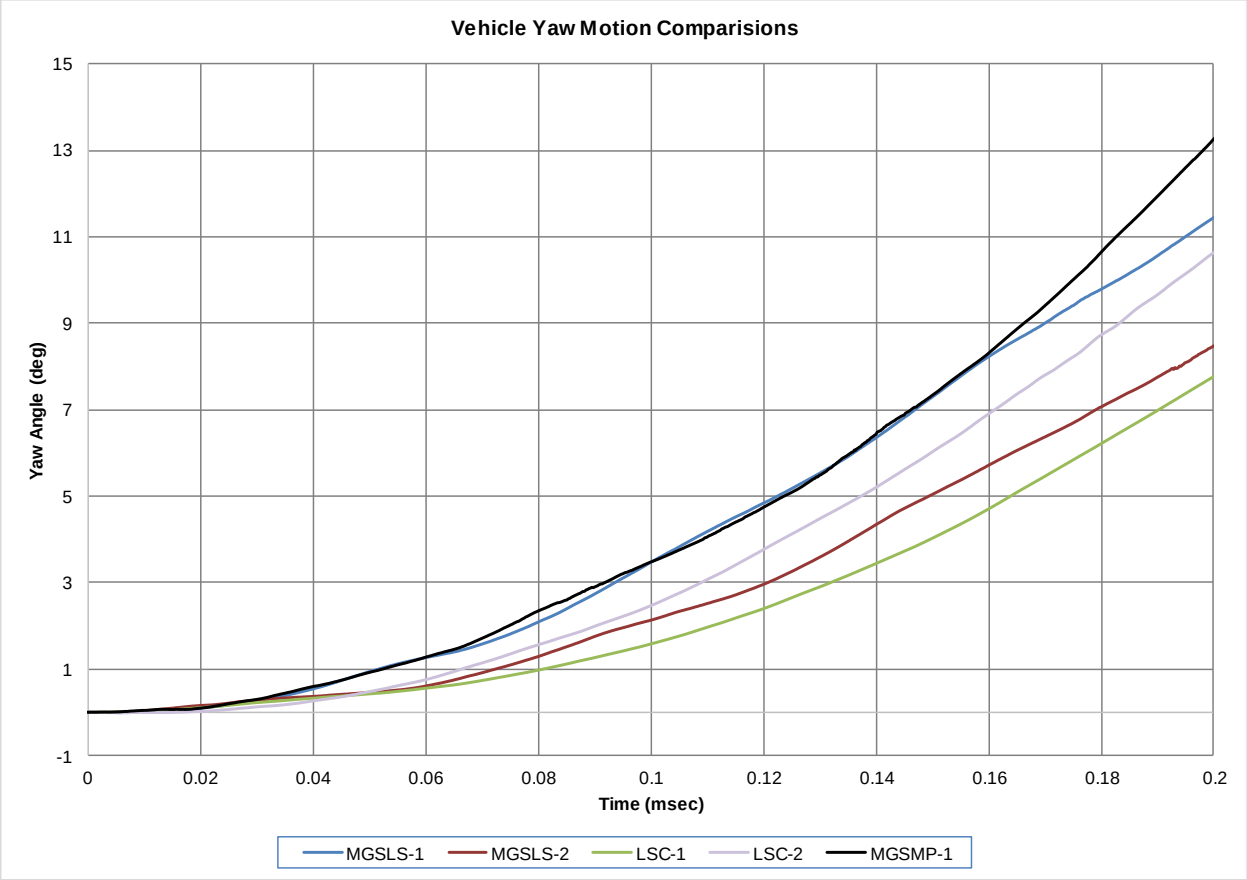

Figure 45. Vehicle Yaw Motion Comparisons

3.3.4 Rail Release from Posts

The final parameter investigated as part of the analysis of the downstream end anchorage failure in test no. MGSLS-2 was release of the guardrail from the posts in the system. The MGS

was designed with the rail splices at the midspan between posts. This change facilitated easier release of the guardrail from the posts due to the bolt head only needing to disengage from a single ply of rail. Release of the rail from the posts prevents the rail from being pulled downward as the posts rotate and aids in maintaining rail height and vehicle capture. The rail release in test no. MGSLS-2 was reviewed to see if it differed from other similar tests.

In test no. MGSLS-2, the rail did not release from the support posts upstream and downstream of impact until after failure of the downstream end anchorage except for the first UBSP downstream of impact. This post disengaged from the rail after it fractured. After failure of the downstream end anchorage, the rail released from all the posts downstream of impact due to the longitudinal translation of the rail. Previous tests of the MGS long-span guardrail and MGS with a single omitted post displayed similar rail release behavior, including test nos. MGSLS-1, LSC-1, LSC-2, and MGSMP-1. In these tests, the guardrail released from the posts early in the impact event, before 0.150 sec after impact, and was limited to posts directly adjacent to impact, similar to test no. MGSLS-2. In test nos. LSC-2 and MGSMP-2, the rail was released from the majority of the upstream posts during the test due to longitudinal rail motion. Similar behavior was noted on the downstream posts in test no. LSC-1 and on both the upstream and downstream posts of test no. MGSLS-1. Thus, rail release of the posts upstream and downstream of impact has been observed in several comparable tests due to longitudinal rail motion. However, this motion occurred much later than the anchor failure in test no. MGSLS-2, and the rail release for test no. MGSLS-2 was very similar to other comparable tests prior to failure of the end anchorage. As such, rail release was not believed to be a factor in the end anchorage failure.

3.4 Overall Results and Conclusions

The analysis of the downstream end anchorage failure in test no. MGSLS-2 included investigation of impact points relative to the unsupported span and the end anchorages, anchorage loads and failure mechanisms, barrier deflection and pocketing prior to failure, post fracture adjacent to the unsupported span, vehicle trajectory, and other factors. These parameters were also compared with other similar or related tests, including test no. MGSLS-1, the MASH crash tests of the original MGS long span, the MGS minimum length testing, testing of the MGS with an omitted post, and testing of the trailing-end anchorage for the MGS.

Results from the analysis found that system deflection and pocketing for test no. MGSLS-2 were increased prior to the anchorage failure when compared to similar testing of the original MGS long span. This finding would suggest that the barrier performance was pushed closer to its limitations than in the previous design. However, loading of the anchorage did not appear to be excessive as anchor loads were similar to test no. MGSLS-1 and lower than observed in several previous tests of the MGS with instrumented anchorages. Examination of the BCT post that failed did not reveal any flaws in the post that may have reduced the post strength, nor was the behavior of the anchorage prior to failure significantly different when compared to other testing. Soil resistive forces in test no. MGSLS-2 compared favorably with previous MASH tests of the MGS, but soil strength comparisons from the full-scale tests of the original MGS long span, test nos. LSC-1 and LSC-2, were not available.

The analysis and comparison was unable to identify a sole root cause for the anchorage failure in test no. MGSLS-2, but several contributing factors were identified.

1. The increased span length of the modified system contributed to increased system deflections and pocketing angles.

2. The critical impact points selected for the evaluation of the original MGS long-span guardrail capacity test and test no. MGSLS-2 were different due to the increased span length. The impact point for test no. MGSLS-2 was closer to the end of the unsupported span and closer to the downstream end anchorage than any previous long span testing. This deviation may have contributed to increased anchor loads and some of the differences in barrier behavior.

3. Review of the fracture of the breakaway posts identified differences in the release of the posts downstream of the unsupported span. Fracture of the breakaway posts on the downstream end of the unsupported span in the increased-length, MGS long-span guardrail occurred later with respect to the relative position of the pickup truck than those in the original long-span guardrail. This is partially due to the differences in the behavior of UBSP as compared to the CRT post and partially due to difference in soil strength. As noted previously, the CRT posts in the original tests displayed post fracture below grade and vertical splitting, which were not possible with the UBSPs. Delayed fracture of the breakaway post relative to the truck position contributes to increased pocketing and rail loading. However, it could not be determined if the difference in post fracture contributed directly to the failure of the downstream anchorage.

4. The timber BCT posts used in the trailing end anchorage have a natural variation in strength. The posts used in the trailing-end terminal for MGSLS-2 were examined before and after the test and displayed no checks, knots, or other flaws that would have reduced the BCT post capacity. However, the natural variation of wood strength could have contributed to a post that was near the lower end of the typical capacity and led to the failure of the anchorage system.

4 POTENTIAL SYSTEM MODIFICATION

While a singular cause for the anchorage failure was not identified, several potential recommendations were developed with respect to improving the performance of the MGS long span with increased span length. These potential recommendations include but are not limited to:

1. Replacing the UBSPs with CRT posts – If the use of UBSPs contributed to the failure of the downstream anchorages due to differences in the breakaway behavior of the posts, reverting to the CRT posts used in the original MGS long-span guardrail may improve the system behavior and aid in preventing end anchorage failure.

2. Extension of the system length to reduce anchorage loads – End anchor loading will decrease as the length of the barrier system increases. Thus, increasing the length of the MGS long span with an increased unsupported span length would reduce anchor loading and reduce the potential for the end anchorage failure. The exact extent to which the barrier system would need to be extended is unknown at this time, and it is noted that large increases in the tested system length may result in barrier lengths that are difficult or impractical to implement in the field.

3. Retest the system with a proprietary steel end anchorage – Various proprietary end terminals and associated end anchorages exist that consist of entirely of steel components. Some of these systems have been evaluated under MASH test designation no. 3-35 in order to evaluate the capacity of the terminal and anchorage through impact of the 2270P vehicle at the beginning of length of need. Reevaluation of the MGS long span with an increased unsupported span length with one of these proprietary steel end anchorages could reduce the potential for anchor failure and release.

4. Await development of the non-proprietary, steel post, trailing end terminal funded in Midwest States Pooled Fund Year 26 and Year 28 – A research effort is currently underway in the Midwest States Pooled Fund program to develop and test a steel post version of the trailing end anchorage used in the evaluation of the MGS long span with increased unsupported span length. This system may offer increased anchor capacity and reduce potential variability due to the use of timber posts in the current end anchorage. Preliminary design of this system is nearly completed and full-scale crash testing is planned under the Year 28 program.

5. Redesign the bearing plate to distribute more load to the foundation tube than the BCT post – The failure of the end anchorage in test no. MGSLS-2 occurred through fracture of the final BCT post near the upper portion of the bearing plate that propagated through the post and released the cable anchor. Redesigning the bearing plate to distribute more load on the foundation tube and less load on the BCT post would reduce the potential for fracture of the BCT post and increase the capacity of the anchorage.

6. Revise the long-span system to incorporate nested guardrail or other rail reinforcement – Incorporation of some form of rail reinforcement could reduce the rail deflection and pocketing that was observed in test no. MGSLS-2, and potentially reduce the loading of the end anchorages. This could be accomplished through the use of nested guardrail or some other form structural reinforcement, such as tubes.

7. Refine the required grading for BCT posts used in the trailing end anchorage to DS-65 – MwRSF has been recommending and full-scale crash testing BCT posts that are SYP Grade No. 1 or better and contain no knots 18 in. (457 mm) above or below ground on the tension face of the post. This recommendation was made to provide for more consistent end anchor capacity and reduce the potential for premature end anchorage failure. Increasing the timber grade requirement for the BCT posts in the end anchorage to DS-65 would potentially improve the capacity and consistency of the end anchorage with minimal modification to the overall barrier system.

Further analysis of these potential improvements, selection of a preferred design, and evaluation of the revised barrier system through full-scale crash tests will be required in order to provide a MASH TL-3 compliant MGS long span with increased span length.

5 SUMMARY AND CONCLUSIONS

An engineering analysis was undertaken to review the downstream end anchorage failure observed in test no. MGSLS-2. The analysis also compared critical aspects of the barrier performance with previous full-scale crash tests that had similar features or increased anchor loading. The analysis found that anchor load, anchor deflection, and anchor stiffness were not significantly different when compared to anchorages from similar tests of the MGS.

Test no. MGSLS-2 with an increased unsupported span length demonstrated higher pocketing angles and rail defections than the original MGS long-span guardrail evaluated in test no. LSC-1, which would indicate that some potential for increased rail loading existed. It was also found that the UBSPs used in test no. MGSLS-2 disengaged when the truck was significantly closer to the post than previous long-span guardrail testing that utilized CRT posts adjacent to the unsupported span. The impact point for test no. MGSLS-2 was compared with other similar tests with respect to its proximity to the first post downstream of impact, its proximity to the first rail splice downstream of impact, and the distance to the downstream end anchorage, but no evidence was found to suggest that the impact point directly contributed to the anchor failure.

The possibility that wood and soil variability contributed to the downstream end anchor failure was also investigated. Variability of the wood material used in the PCB posts was noted as a potential factor, but examination of the fractured posts did not indicate any issues with that would have affected the strength and capacity of the end anchorage. Review of static soil test data from test no. MGSLS-2 and comparable tests found that the soil response from test no. MGSLS-2 would not have been expected to produce more severe loading of the end anchorage. Comparisons of vehicle trajectory and rail release from the posts in test no. MGSLS-2 showed no potential for increased anchor loading or failure, but it did denote different system response as compared to previous testing.

The results of this analysis and conclusions regarding potential causes of the anchor failure suggested that there was no identifiable root cause for anchor failure, but the pocketing and deflection suggest that barrier system may have been pushed near its limits. It was noted that certain factors may have contributed to the anchor failure, including increased span length, location of in the impact point, differences in the breakaway post behavior adjacent to the unsupported span, and natural variation in wood strength.

Following the analysis, several potential design modifications were noted for improving the barrier system and reducing the potential for failure of the end anchorage. However, it was noted that further analysis of these potential improvements, selection of a preferred design, and evaluation of the revised barrier system through full-scale crash tests will be required to fully evaluate the system to MASH TL-3 criteria.

6 REFERENCES

1. Hirsch, T.J. and Beggs, D., *Use of Guardrails on Low Fill Bridge Length Culverts*, Research Report No. 405-2 (F), Texas Transportation Institute, College Station, TX, August 1987.

2. Hirsch, T.J. and Beggs, D., *Use of Guardrails on Low Fill Bridge Length Culverts*, Transportation Research Record No. 1198, Transportation Research Board, National Research Council, Washington, D.C., 1988

3. Pfeifer, B.G. and Luedke, J.K., *Safety Performance Evaluation of a Nested W-Beam with Half-Post Spacing Over a Low-Fill Culvert*, Report No. TRP-03-36-92, Midwest Roadside Safety Facility, University of Nebraska-Lincoln, Lincoln, Nebraska, March 1993.

4. Memorandum on W-Beam Guardrail over Low-Fill Culverts, September 9, 1991, File Designation HNG-14, Federal Highway Administration (FHWA), Washington, D.C., 1991.

5. Mak, K.K., Bligh, R.P., Gripne, D.J., and McDevitt, C.F., *Long-Span Nested W-Beam Guardrails over Low-Fill Culverts*, Transportation Research Record No. 1367, Transportation Research Board, National Research Council, Washington, D.C., 1992.

6. Buth, E.C., Bullard, L.D., and Menges, W.L., *NCHRP Report 350 Test 3-11 of the Long-Span Guardrail with 5.7 m Clear Span and Nested W-beams over 11.4 m*, Report No. 405160-1-1, Texas Transportation Institute, College Station, TX, July 2006.

7. Polivka, K.A., Bielenberg, B.W., Sicking, D.L., Faller, R.K., and Rohde, J.R., *Development of a 7.62-m Long Span Guardrail System*, Report No. TRP-03-72-99, Midwest Roadside Safety Facility, University of Nebraska-Lincoln, Lincoln, Nebraska, April 6, 1999.

8. Polivka, K.A., Bielenberg, B.W., Sicking, D.L., Faller, R.K., Rohde, J.R., and Keller, E.A., *Development of a 7.62-m Long Span Guardrail System - Phase II*, Report No. TRP-03-88-99, Midwest Roadside Safety Facility, University of Nebraska-Lincoln, Lincoln, Nebraska, August 13, 1999.

9. Faller, R.K., Sicking, D.L., Polivka, K.A., Rohde, J.R., and Bielenberg, R.W., *A Long-Span Guardrail System for Culvert Applications*, Paper No. 00-0598, Transportation Research Record No. 1720, Transportation Research Board, Washington, D.C., 2000.

10. Polivka, K.A., Faller, R.K., Sicking, D.L., Rohde, J.R., Reid, J.D., and Holloway, J.C., *NCHRP 350 Development and Testing of a Guardrail Connection to Low-fill Culverts*, Report No. TRP-03-114-02, Midwest Roadside Safety Facility, University of Nebraska-Lincoln, Lincoln, Nebraska, November 1, 2002.

11. Polivka, K.A., Faller, R.K., and Rohde, J.R., *Guardrail Connection for Low-fill Culverts*, Paper No. 03-4421, Transportation Research Record No. 1851, Transportation Research Board, Washington, D.C., 2003.

12. Bielenberg, R.W., Faller, R.K., Rohde, J.R., Reid, J.D., Sicking, D.L., Holloway, J.C., Allison, E.M., and Polivka, K.A., *Midwest Guardrail System for Long-Span Culvert Applications*, Report No. TRP-03-187-07, Midwest Roadside Safety Facility, University of Nebraska-Lincoln, Lincoln, Nebraska, November 16, 2007.

13. Bielenberg, R.W., Faller, R.K., Sicking, D.L., Rohde, J.R., and Reid, J.D., *Midwest Guardrail System for Long-Span Culvert Applications*, Paper No. 07-2539, Transportation Research Record No. 2025, Transportation Research Board, Washington, D.C., 2007.

14. Meyer, D.T., Reid, J.D., Faller, R.K., Bielenberg, R.W., Lechtenberg, K.A., *Increased Span Length for the MGS Long-Span Guardrail System Part II: Full-scale Crash Testing*, Research Report No. TRP-03-339-16, Midwest Roadside Safety Facility, University of Nebraska-Lincoln, Lincoln, Nebraska, April 7, 2017.

15. *Manual for Assessing Safety Hardware (MASH)*, American Association of State Highway and Transportation Officials (AASHTO), Washington, D.C., 2009.

16. Weiland, N.A., Reid, J.D., Faller, R.K., Bielenberg, R.W., *Increased Span Length for the MGS Long-Span Guardrail System*, Report No. TRP-03-310-14, Midwest Roadside Safety Facility, University of Nebraska-Lincoln, Lincoln, Nebraska, December 17, 2014.

17. Lingenfelter, J.L., Rosenbaugh, S.K., Bielenberg, R.W., Lechtenberg, K.A., Faller, R.K., and Reid, J.D., *Midwest Guardrail System (MGS) with an Omitted Post*, Report No. TRP-03-326-16, Midwest Roadside Safety Facility, University of Nebraska-Lincoln, Lincoln, Nebraska, February 22, 2016.

18. Weiland, N.A., Reid, J.D., Faller, R.K., Sicking, D.L., Bielenberg, R.W., and Lechtenberg, K.A., *Minimum effect Guardrail length for the MGS*, Report No. TRP-03-276-13, Midwest Roadside Safety Facility, University of Nebraska-Lincoln, Lincoln, Nebraska, August 12, 2013.

19. Mongiardini, M., Faller, R.K., Reid, J.D., Sicking, D.L., Stolle, C.S., and Lechtenberg, K.A., *Downstream Anchoring Requirements for the Midwest Guardrail System*, Report No. TRP-03-279-13, Midwest Roadside Safety Facility, University of Nebraska-Lincoln, Lincoln, Nebraska, October 28, 2013.

20. Stolle, C.S., Reid, J.D., Faller, R.K., Mongiardini, M., *Dynamic strength of a modified W-beam BCT trailing-end termination system*, International Journal of Crashworthiness, Vol.20, Iss. 3, 2015.

21. Gutierrez, D.A., Reid, J.D., Faller, R.K., Bielenberg, R.W., Lechtenberg, K.A., *Development of a MASH TL-3 Transition between Guardrail and Portable Concrete Barriers*, MwRSF Research Report No. TRP-03-300-14, Midwest Roadside Safety Facility, University of Nebraska-Lincoln, Lincoln, Nebraska, June 26, 2014.

22. Rosenbaugh, S.K., Lechtenberg, K.A., Faller, R.K., Sicking, D.L., Bielenberg, R.B., and Reid, J.D., *Development of the MGS Approach Guardrail Transition Using Standardized Steel Posts*, Report No. TRP-03-210-10, Midwest Roadside Safety Facility, University of Nebraska-Lincoln, Lincoln, Nebraska, December 21, 2010.

END OF DOCUMENT